1983

An examination of techniques for the removal of NOx and NOx/SOx from flue gases.

Kam Foon. Chan
University of Windsor

CANADIAN THESES ON MICROFICHE

I.S.B.N.

THESES CANADIENNES SUR MICROFICHE

National Library of Canada
Collections Development Branch

Canadian Theses on
Microfiche Service

Ottawa, Canada
K1A 0N4

Bibliothèque nationale du Canada
Direction du développement des collections

Service des thèses canadiennes
sur microfiche

NOTICE

The quality of this microfiche is heavily dependent upon the quality of the original thesis submitted for microfilming. Every effort has been made to ensure the highest quality of reproduction possible.

If pages are missing, contact the university which granted the degree.

Some pages may have indistinct print especially if the original pages were typed with a poor typewriter ribbon or if the university sent us a poor photocopy.

Previously copyrighted materials (journal articles, published tests, etc.) are not filmed.

Reproduction in full or in part of this film is governed by the Canadian Copyright Act, R.S.C. 1970, c. C-30. Please read the authorization forms which accompany this thesis.

THIS DISSERTATION
HAS BEEN MICROFILMED
EXACTLY AS RECEIVED

AVIS

La qualité de cette microfiche dépend grandement de la qualité de la thèse soumise au microfilmage. Nous avons tout fait pour assurer une qualité supérieure de reproduction.

S'il manque des pages, veuillez communiquer avec l'université qui a conféré le grade.

La qualité d'impression de certaines pages peut laisser à désirer, surtout si les pages originales ont été dactylographiées à l'aide d'un ruban usé ou si l'université nous a fait parvenir une photocopie de mauvaise qualité.

Les documents qui font déjà l'objet d'un droit d'auteur (articles de revue, examens publiés, etc.) ne sont pas microfilmés.

La reproduction, même partielle, de ce microfilm est soumise à la Loi canadienne sur le droit d'auteur, SRC 1970, c. C-30. Veuillez prendre connaissance des formules d'autorisation qui accompagnent cette thèse.

LA THÈSE A ÉTÉ
MICROFILMÉE TELLE QUE
NOUS L'AVONS REÇUE

NL-339 (r. 82/08)

Canada

AN EXAMINATION OF TECHNIQUES FOR THE REMOVAL OF NO_x AND NO_x/SO_x FROM FLUE GASES

by

Kam Foon Chan

A Thesis
submitted to the
Faculty of Graduate Studies and Research
through the Department of
Chemical Engineering in Partial Fulfillment
of the requirements for the Degree
of Master of Applied Science at
the University of Windsor

Windsor , Ontario, Canada

1983

ABSTRACT

The adverse effects of NO_x on human health and the environment are summarized in this study. A review of the NO_x control technologies indicates that the selective catalytic reduction methods (SCR) are more suitable for cleaner flue gases containing low levels of emitted particulates and SO_x. For higher sulphur and particulate emission processes such as coal-firing, the wet, simultaneous NO_x/SO_x absorption methods are more applicable than other existing technologies.

On the basis of the two-film theory, new absorption models are derived for predicting the rate of absorption of NO_x/SO_x in a packed column for :

1. physical absorption with water.
2. chemical absorption with mixed sodium hydroxide and sodium chlorite sclution.

These models use a liquid residence time distribution function in a packed column as a means of accounting for the semi-stagnant liquid pools in such units.

The derived physical model is not limited to the NO_x/SO_x absorption problem but can be extended to any gaseous-liquid reaction in such columns. However, the chemical absorption model is restricted to the NO_x/SO_x - ($NaOH + NaClO_2$) system because of the reaction kinetics involved.

Most previous experimental studies on NO_X/SO_X absorption were either semi-batch operations or restricted to single NO_X or SO_X absorption. Experimental studies on single or combined NO_X /SO_X removal in packed columns under flow conditions are rarely found. Literature values, therefore, are not available to verify these new models. Experimental studies aimed at collecting these data are proposed.

ACKNOWLEGEMENTS

The author wishes to express his gratitude to Dr. A. W. Gnyp for his guidance , for providing information and helpful suggestions during this study. During the preparation of this draft, Dr. A. W. Gnyp also kindly helped to proofread the manuscript.

Thanks are also extended to the Air Resources Branch of The Ontario Ministry of The Environment for financial support of this study. Gratitudes are also extended to Professor M. B. Powley for his helpful discussions on absorption theory.

TABLE OF CONTENTS

LIST OF FIGURES

LIST OF TABLES

I. INTRODUCTION

Several stable oxides of nitrogen are known. Those recognized as important air pollutants are nitric oxide (NO) and nitrogen dioxide (NO_2) which are collectively referred to as NO_x.

Extensive studies of the effects of NO_x exposures on different species have shown that most oxides of nitrogen are toxic to humans, animals, and plants. Concentrations of nitrogen dioxide as low as 10 - 20 ppm have been shown to cause persistent pathological changes in animals after continuous exposures for 3 to 4 months [1]. These health effects emphasize the need for controlling the emissions of NO_x into the atmosphere from man-made sources in most countries. Although the production of nitrogen oxides by naturally occurring processes is much greater than what results from man-made sources, the naturally occurring oxides of nitrogen are well distributed over the globe at low concentrations. Consequently they cause less hazards to the environment. On the other hand the oxides from man-made sources are concentrated locally in urban areas at levels ranging from 0.04 to 0.077 ppm [2,3]. The localized concentrations of NO_x are assumed to increase as human activities increase.

Figure 1-1 depicts potential NO_x emissions in the United States up to the year 2000.

The major man-made sources of nitrogen oxides are stationary combustion facilities and automobiles. Typical NO_x emission levels from industrial boilers are shown in Table 1-1. Table 1-2 summarizes the calculated equilibrium concentrations of NO_x for four different fuels as determined by Iya [6]. Iya indicates that more than 90 percent of the nitrogen oxides are inactive nitric species at concentrations of several hundred ppm. These colorless nitric oxides in the presence of air will, given sufficient time, oxidize to nitrogen dioxide. Nitrogen dioxide is a reddish-brown, toxic gas which, in the presence of certain hydrocarbons and sunlight, is a precursor for photochemical smog and acid aerosols.

Considerable research has been directed towards the development of systems for removing nitric oxides by wet and dry methods.

The wet scrubbing techniques are of major concern in Japan, while the dry methods, including catalytic reduction of NO into N_2 and O_2 and combustion modification to decrease the formation of NO_x, are important in the United States. Each of these approaches has its own limitations with respect to the handling of NO_x problems. For example, boiler modifications are limited to less than 50 percent reduction in NO_x emissions while the catalytic reduction processes

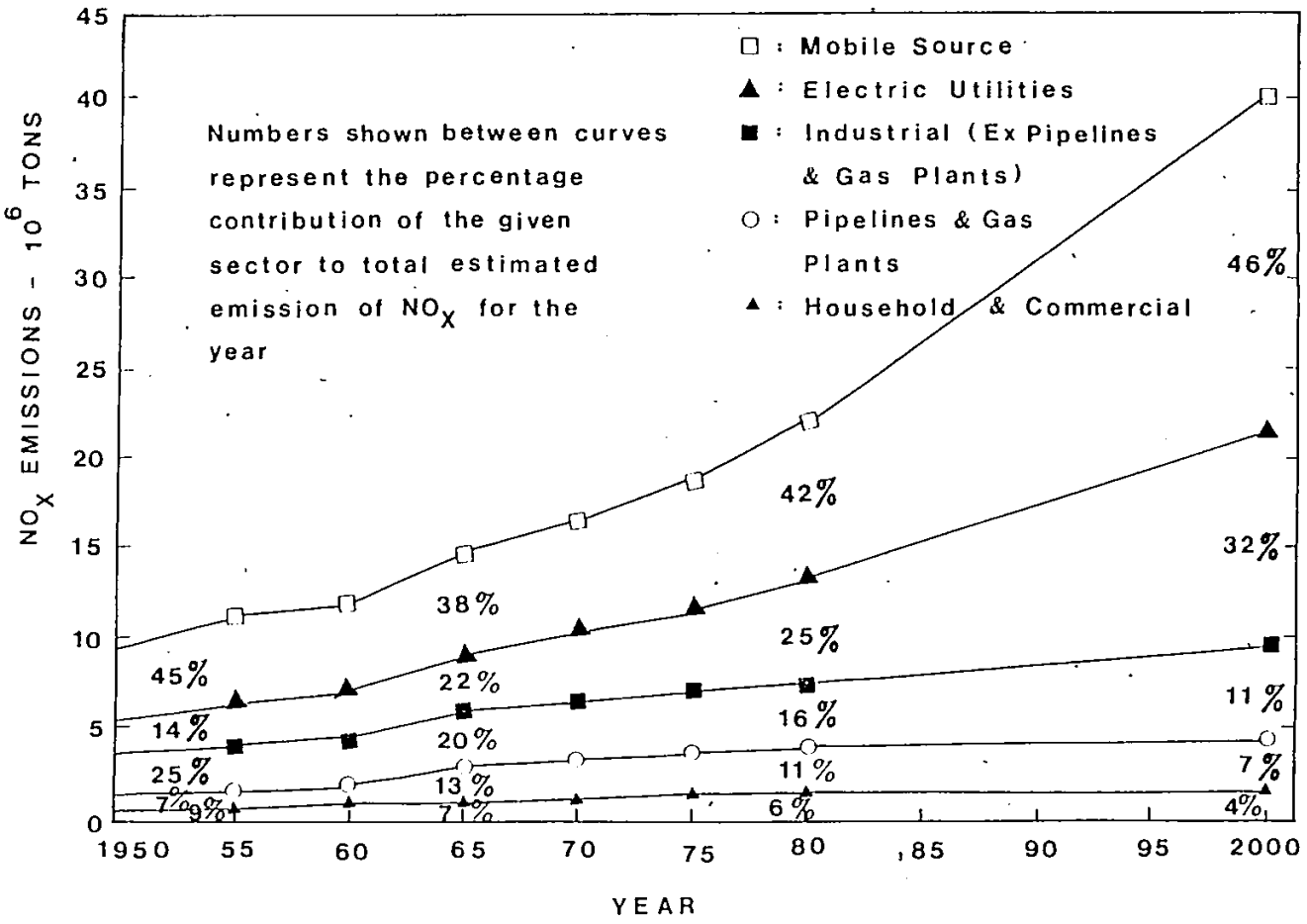

Figure 1-1 : Potential NO_X Emissions in the U.S.A. – Culmulative (Median Economic Trends) (4)

TABLE 1.1

Typical NO_X Emission Levels For Industrial Boilers [5].

	NO_X EMISSION LEVEL (PPM IN STACK GAS)			
	Without Controls		With Controls	
Fuel Type	Range	Average	Range	Average
Natural Gas	50-1000	200	50-350	110
Oil	65- 650	280	150-365	210
Coal	164-1500	475	200-700	370

TABLE 1.2

NO_X Equilibrium Concentrations For Different Fuels [5].

	Inlet Gas Composition % Volume					Equilibrium Combustion		
Type of flame	CH_4	C_2H_2	C_2H_4	H_2	Air	Temp. F	NO ppm	NO_2 ppm
CH_4/Air	4.5	-	-	-	95.5	2039	520	2.8
C_2H_2/Air	-	3.0	-	-	97.0	2149	804	3.8
C_2H_2/Air	-	-	3.0	-	97.0	2208	880	3.5
H_2/Air	-	-	-	14.	86.0	2075	594	3.1

are particularly sensitive to dust and plugging. Also, the catalyst base material may be subject to chemical attack. Unlike the dry methods, wet NO_x removal processes have the potential of removing SO_x -NO_x simultaneously. In addition, the wet processes are relatively insensitive to flue gas particulate matter and high SO_x content. As more stringent regulations concerning NO_x emissions are adopted, better flue gas treatment will be necessary. Table 1-3 lists the wet NO_x abatement techniques currently in use in Japan.

In spite of the widespread application of wet scrubbing techniques to the control of NO_x emissions, the removal of NO from gas mixtures by liquid absorbents is practically unsolved. This chief constituent of NO_x is so inactive that it is emitted without any abatement into the atmosphere. Takeuchi and co-workers [7], in a series of experiments on absorption of NO in aqueous sodium sulfite, have found that the rate of NO absorption is very slow at parts per-million concentrations. This behavior suggests a need for a catalyst that will enhance the reaction in the liquid phase. Otherwise it may be possible to remove NO after converting it into NO_2 by a gas phase reaction. The initial suggestion is the focus of research carried out by Teramoto et al.[8], Hikita [9] and many other researchers [10, 11, 12]. Although substantial experimental work has been carried out by these investigators, a promising scrubbing solution for NO absorption has not yet been found. Comparatively little attention

TABLE 1-3

NO_x Abatement Techniques Currently in Use in Japan (5)

Process	Description	Advantages	Disadvantages
Reduction by Sodium Sulfite (CCIC-JECCO Process)	Sodium Sulfite reduces NO_x to N_2.	NO_x reduced from 3000 to 50 ppm. Sodium sulfite usually available from desulfurization processes.	Large flow rates and excess O_2 hinders reduction.
Sodium Scrubbing (Fujikasui Process)	ClO_2 oxidizes NO to NO_2. NO_2 scrubbed with $NaClO_2$.	Up to 90% NO_x removal. Low cost, easy operation.	SO_2 hinders RXN - must be prescrubbed. Wastewater treatment required for NaCl & $NaNO_3$ from scrubber.
Alkali Permanganate (MON Process)	NO_x & SO_2 absorbed and oxidized with alkali permanganate to form alkali nitrate and sulfate. Manganese dioxide precipitate is reduced for reuse.	Nitrate is used for fertilizer. Pilot plant shows 90% removal of NO_x. No waste material.	Alkali KOH and permanganate production is expensive.
Sodium-Potassium Permanganate (Nissan Process)	70-80% of NO_x removal in scrubber with NaOH. Off gas is oxidized with permanganate and NO_2 absorbed with NaOH. Two scrubber process.	High NO_x removal and flexible operation. NO_x off gas reduced to less than 100 ppm.	Na_2NO_3 waste treatment is required.
Alkali Scrubbing (ChinKo Process)	NO_x is scrubbed with NaOH for 50% removal. Off gas sent to packed tower containing granular alumina sprayed with NaOH and $NaClO_2$-dried. 95% NO_x is removed with products	High removal of NO_x (95%).	$NaClO_2$ is expensive.

TABLE 1-3 (Continued)

NO_x Abatement Techniques Currently in Use in Japan (5)

Process	Description	Advantages	Disadvantages
	of $NaNO_3$. NaCl & gaseous ClO_2.		
Sodium Scrubbing (Sun Mec Sv Process)	High NO_x concentration gas, such as from pickling plants, is first scrubbed with NaOH. Off gas of 1000-3000 ppm NO_x is oxidized with a catalyst, steam sprayed to produce HNO_3 which is subsequently washed with NaOH.	Easy operation and maintenance. NaOH prescrubbed NO_x is reduced to 1000-3000 ppm and further reduced to 200 ppm.	Process not suited for flue gas treatment. Wastewater containing $NaNO_3$.
Alkali Scrubbing (Kyowa Kako Process)	Waste gases from pickling plants are first scrubbed with NaOH, off gas is oxidized with hydrogen peroxide and then washed with alkali hydrogen sulfide or alkali sulfide.	High NO_x removal ratio. 4000 ppm NO_x reduced to 50 ppm.	Difficult wastewater treatment and sludge disposal.
Sodium Scrubbing (Ube Process)	Nitric acid plant process gas NO_2/NO ratio is adjusted to 1.0. The gas is scrubbed with NaOH to form $NaNO_2$ and $NaNO_3$.	Simple process, low investment and operating costs. NO_x reduced to 200 ppm.	Produces large quantities of $NaNO_2$ and $NaNO_3$.

Other Alkali Scrubbing Processes

Mitsubishi Heavy Industries.

Pickling plant gases are first scrubbed with water to recover nitric acid, off gas is scrubbed with NaOH. NO_x reduced from 700-2100 ppm to 280-490 ppm.

Nishinaka Industries Process.

NO is oxidized to NO_2 in an activated carbon layer and then scrubbed with NaOH to form $NaNO_2$ and $NaNO_3$.

has been given to the wet, simultaneous removal of NO_X/SO_X in a packed column. Experiments focussing on this problem are rarely found in the literature.

The potentially toxic effects of NO_X on human health and the environment have initiated some NO_X emission control policies in the U.S. and Japan but not in this country.

1.1 OBJECTIVES

The present work is divided into two parts. The first phase summarizes recent key findings concerning :

1. the possible impact of NO_X on human health and the environment in this country.
2. the improvement of NO_X control technologies during recent commercial tryouts.
3. the evaluation of the most promising methods available for NO_X emission control for coal-firing processes.

On the basis of the evaluation of NO_X control technologies in part one, the second phase of this study was undertaken to

1. develop absorption models for predicting absorption rates in packed columns.
2. design an absorption experiment for the study of NO_X/SO_X emission control.

1.2 METHOD OF APPROACH

To initiate the study of the impact of NO_x emissions in this country a comprehensive review of the effects of NO_x on human health and the environment was carried out. Then, a critical evaluation of the existing control technologies was completed. On the basis of this evaluation, an attempt has been made to develop a viable process for removing NO_x/SO_x simultaneously.

REFERENCES

1. Davidson J.T., The Anatomical and Physiological Changes of Rabbits Exposed to NO_2 - Presented at 59 th Annual Meeting, Air Pollution Control Assoc., San Francisco, pp.20-24, (June 1966).

2. Environmental Health Criteria, Oxides of Nitrogen. WHO Publication, 4, (1977).

3. Stern A.C., The Effects of Air Pollution. Academic Press, 3rd Edition, pp.13, (1977).

4. Bartok W., Crawford A.R., Cunningham A.R., Hall H.J., Manny E.H., and Skopp A., Systems Study of Nitrogen Oxide Control Methods for Stationary Sources. Final Report - Vol.II, Esso Research and Engineering Company, Government Research Laboratory, (Nov. 20, 1969).

5. Siddiqi A.A., Control NO_x Emissions from Fixed Fireboxes. Hydrocarbon Processing, pp.94 - 97, (Oct. 1976).

6. Iya K.Sridhar, Reduce NO_x in Stack Gases. Hydrocarbon Processing, pp.163 - 164, (Nov. 1972).

7. Takeuchi H., Ando M., and Kizawa N., Absorption of Nitrogen Oxides in Aqueous Sodium Sulfite and Bisulfite Solutions. Industrial Engineering Chemistry, Process Design Development, 16, NO.3, pp.303-308, (1977).

8. Teramoto M., Hiramine S., Shimada Y., Sugimoto Y., and Teranishi H., Absorption of Dilute Nitric Monoxide in Aqueous Solutions of Fe(II)-EDTA and Mixed Solutions of Fe(II)-EDTA and Na_2SO_3 - Journal of Chemical Engineering of Japan, 11, No.6, pp.450-457, (1978).

9. Hikita H., Asai S., Ishikawa H., Okamoto T., Sakamoto S., and Kitagawa M., Kinetics of Absorption NO into Aqueous Na_2SO_3 Solutions Containing Fe(III)-EDTA-Na and $Fe_2(SO_4)_3$ Journal of Chemical Engineering of Japan, 11, No.5, pp.360-365, (1978).

10. Sada E. and Kumazawa H., Absorption of NO in Aqueous Solutions of Fe(III)-EDTA Chelate and Aqueous Slurries of $MgSO_3$ with Fe(III) -EDTA Chelate. Industrial Engineering Chemistry, Process Design Development, 20, No.1, pp.46-49, (1981).

11. Lefers J.B., Bleek van den C.M., and Berg van den P.J., The Oxidation and Absorption of Nitrogen Oxides in Nitric Acid in Relation to The Tail Gas Problem of Nitric Acid Plants. Chemical Engineering Science, 35, pp.145-153, (1980).

12. Baveja K.K., Babba Rao D., and Sarkar M.K., Kinetics of Absorption of Nitric Oxide in Hydrogen Peroxide Solutions. Journal of Chemical Engineering Japan, 12, No.4, pp.322-325, (1979).

II. LITERATURE REVIEW

The possible hazards to vegetation and human health resulting from emission of NO_X into the atmosphere are reviewed in this chapter. Fixation principles, sources of NO_X production and current control techniques are also discussed comprehensively. Recent findings concerning improvements to NO_X control techniques are also reported. This discussion is intended to explore the current situations with respect to trends in NO_X emissions and the most promising control techologies for abatement of NO_X emissions at coal-fired thermal generating stations in Ontario.

2.1 ENVIRONMENTAL EFFECTS OF NO_X

The effects of NO_X on the environment are quite varied because it is corrosive to materials and toxic to humans and other forms of life. The oxides of nitrogen also play an important role in smog formation. It is now well documented that NO_X is an essential component in the formation of photochemical oxidants such as ozone. It can also be converted into nitric acid, one of the two principal sources of acid precipitation.

2.1.0.1 Vegetation

According to most findings [1,2,3,4,5,6,7,8,], nitrogen oxides are toxic to vegetation. Many plants can metabolize low concentrations of NO_x, however, higher concentrations reduce growth and seed fertility. As observed by Fujiwara [1], Troiano and Leone [4], Durmishidze and Nutsubidze [5], Capron and Mansfield [7], and Li et al. [8], exposure of tomato plants, tulips, peas, aspen, apple, mulberry, wild pear, Russian olive, domestic cherry, plum and grapevines, for 5 to 30 minutes to atmospheres containing oxides of nitrogen at concentration levels below 1 ppm resulted in the incorporation of nitrogen into plant amino acids and inhibition of the rate of photosynthesis. An 8 hour fumigation of elm and mountain-ash with low NO_2 concentrations in the studies by Popov [6] indicated that NO_2 decreased the folim content of chlorophyll and carotenoids. The damage gradually increased during the growth season. A similar study [3] on several potted-woody and perennial plants showed that injury appeared after 1 hour of fumigation with 12 ppm NO_2.

2.1.0.2 Acid Rain [10,23]

In addition to the toxicity on vegetation, NO_x emissions also affect the environment by contributing substantially to the acid rain problem. Through a series of complex atmospheric reactions, nitrogen oxides mix with water vapor in the air to form a weak nitric acid solution which is one of

the major sources of acid rain. Rainfall tested in various parts of the country has become much more acidic over the past years. Nearly half [23] of the present acidity is due to nitric acid. Although the acidity of precipitation in Ontario varies considerably, most of the province is affected to some extent. Precipitation acidity is generally highest in southern and south-central Ontario, where much of the fall-out comes from air masses that have passed over industrial sources of sulphur and nitrogen oxides in both the United States and Ontario. Figure 2-1 shows U.S. sources of acid precipitation falling on Canada.

According to the Ontario Ministry of the Environment [10], 140 lakes in the province, mostly in the Sudbury region, have been acidified. A further estimate suggests that 48,500 additional lakes will not be able to tolerate continuing acid inputs for any extended period of time. At current rates of acid deposition, all of these lakes could be dead within the next 20 years. In the Muskoka-Haliburton region, where the lakes are particularly susceptible (poorly buffered) and precipitation acidities are extremely high, the life expectancy of many lakes is ten years or less. Other areas of Canada, such as Nova Scotia, Quebec and the other Maritime Provinces, experience similar effects. This acid rainfall problem, caused by uncontrolled NO_X/SO_X emissions, is not limited to the loss of aquatic life in thousands of Ontario lakes. It is also known to contribute to the deteri-

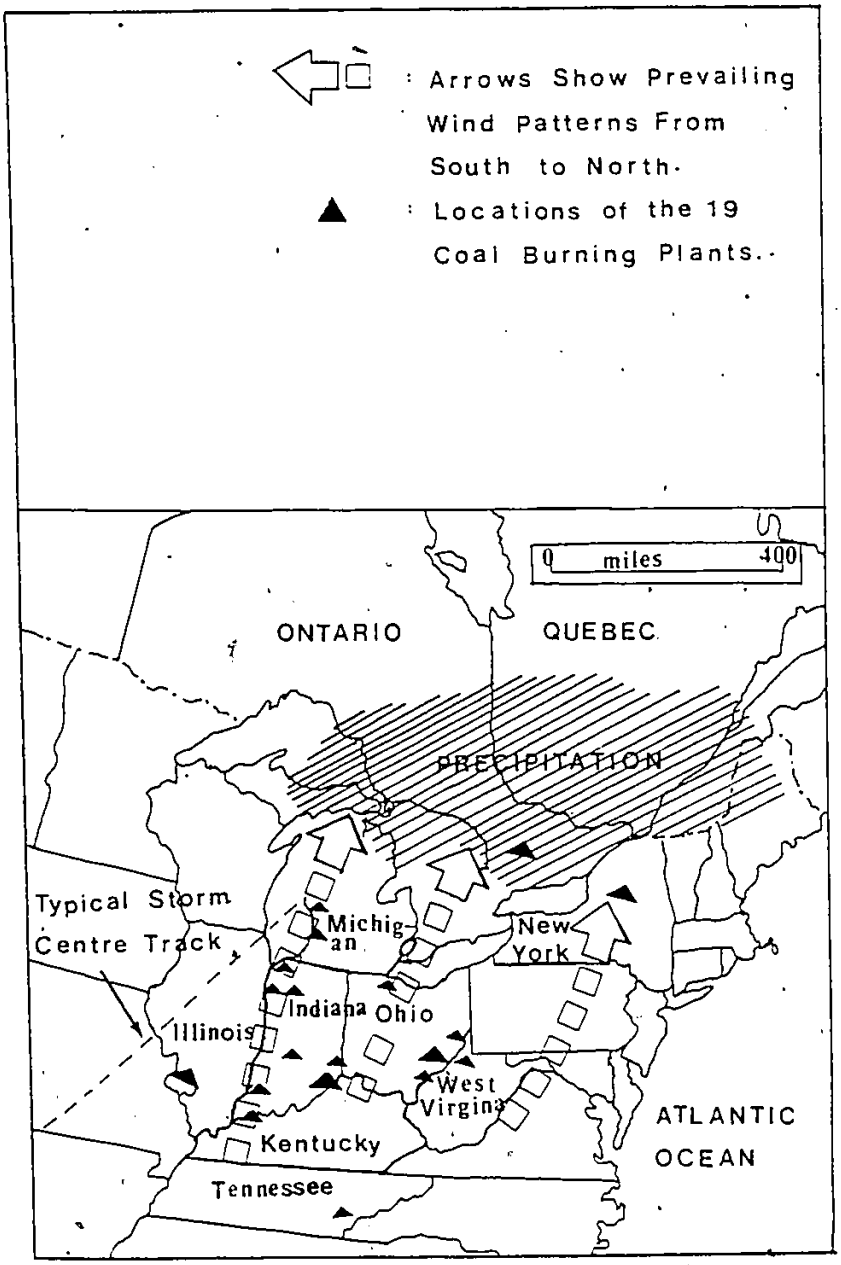

Figure 2-1 : Map Shows Sources of Acid Precipitation Falling on Canada (9)

oration of buildings, paint and metal structures. There is some evidence that its indirect effects endanger human-health as well [10].

2.1.0.3 Human Health

Concern about the health effects of NO_X has led some affected jurisdictions, most notably in the United States and Japan, to control emissions into the atmosphere. Figure 2-2 compares the NO_X ambient standards in the United States and Japan for the 1970-1978 period. Of the two countries, the Japanese ambient standards for NO_2 are about two times lower than the American. Apart from the acid rain problem, NO_X reacts with hydrocarbons [12] in the presence of sunlight to form photochemical oxidants commonly known as smog. When inhaled deeply into the lungs, this smog irritates the respiratory system and can seriously aggravate asthma and other respiratory problems [13,14,15,16,17,18]. Coughing, eye irritation, headaches and throat pain are commonly experienced during exposure to smog.

Continuous exposure to NO_X by itself at low concentrations (< 1 ppm) has been shown to be an area of concern [18]. The risks of acute respiratory disease and susceptibility to chronic respiratory infection is believed to increase [18]. Occasional exposure to low levels of NO_2 can irritate the eyes and skin. At high concentrations, this pollutant can be fatal. Although the toxicity of NO_X is pri-

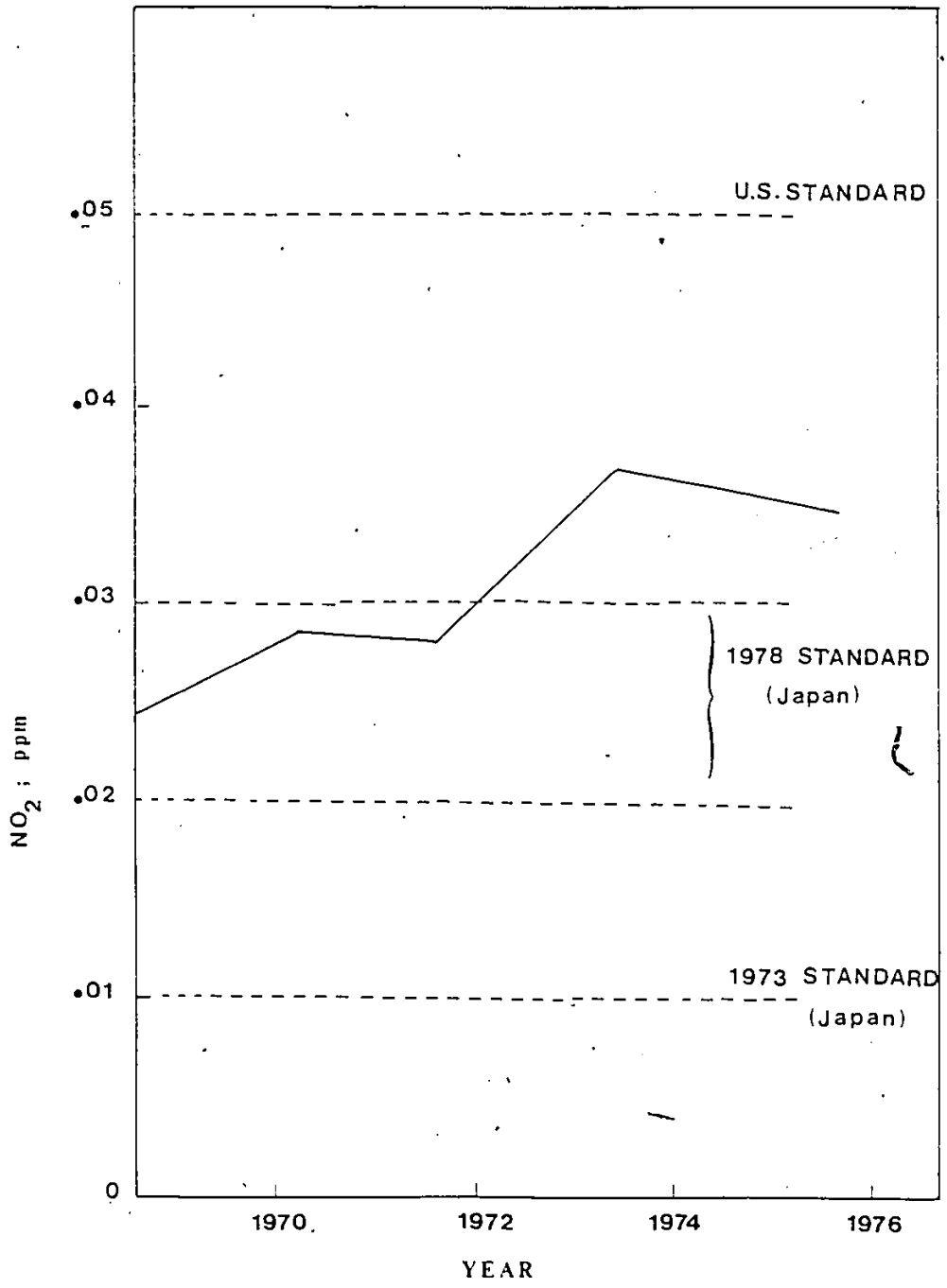

Figure 2-2 : Ambient NO_2 Standards and Concentrations ; Yearly Average (11).

marily on the lungs, effects have also been observed on growth, body weight, immobilized reactions, reproduction and the central nervous system. The health effects have been obtained from studies on various mammalian species and extrapolated to humans.

Although there are limited amounts of published data describing direct studies on human subjects, there is some documentation that exposure of humans to NO_2 concentration at levels ranging from 0.2 to 2 ppm for one to two hours will produce eye irritation [19]. Continuous long term exposures to low levels of NO_2 also lead to respiratory problems in humans. Although nitrogen oxides appear to pose some dangers to human health, the extent and precise nature of these threats are not well known. For example, nitrogen dioxide has been found to contribute to heart, lung, liver, and kidney damage [10,13,18].

Any assessment of the overall human health effects of NO_X is complicated by the epidemiological difficulty of distinguishing the effects of NO_X from those related to sulphur dioxide and particulate emissions from the same contributory sources [10]. Nitrogen dioxide and nitrate particulate matter have both been linked to human health problems but the Federal Department of National Health and Welfare, which is responsible for administering the Clean Air Act, has concluded that NO_X/SO_X are not a significant hazard to human health at the ambient concentrations currently measured in

Canada. It is generally conceded that there is an absence of scientific certainty about the extent and severity of the human health effects of nitrogen dioxide, nitrate particulate matter and acidic precipitation singly or in combination. However, it has been concluded that the concentration of NO_2 for brief exposures should not exceed 3 ppm (for one hour exposure) and for long term continuous exposure, it should not exceed 0.5 ppm.

2.2 GENERAL CHEMISTRY OF NO_X AND ITS SOURCES

The chemistry of the atmospheric reactions involving NO_X is important to NO_X emission control technology. Since NO_X formation from thermal fixation and from nitrogen containing fuel combustion represents a significant portion of the NO_X burden these processes have been reviewed in detail. The relative significance of the various emission sources and the regional variations in NO_X emission profiles are also examined. This discussion is presented to illustrate the trends in NO_X emissions and the need for flue gas treatment (FGT) in the province of Ontario.

2.2.1 General Chemistry of NO_X

2.2.1.1 Atmospheric Reactions of NO_X - Smog Formation [12, 20]

The bulk of the NO_X emitted from both stationary and mobile sources is in the form of nitric oxide (NO). While being transported from an emission source to a sink or recep-

tor, the emitted NO may undergo a series of complex transformations to urban smog. Although much work has been done recently to develop a better understanding of the mechanisms involved in the formation of various atmospheric pollutants, considerable scope remains in the areas of

1. quantification of the various reactive chemical species present in urban air masses and the reactive intermediates for key component formation.
2. identification of the specific chemical mechanisms whereby important chemical species are formed.
3. quantification of the important variables which affect the rates of formation and disappearance of important chemical species.

The role of NO_x in the formation of smog can be summarized by the following photolytic cycle [20] :

Step 1. The conversion of NO to NO_2 .

NO → Path 1 (slow)

Reaction with molecular oxygen

$$2NO + O_2 \longrightarrow 2NO_2 \qquad \text{.....(2-1)}$$

NO → Path 2 (fast)

i. Reaction with hydroperoxy radical

$$NO + HO_2 \longrightarrow NO_2 + OH \qquad \text{.....(2-2)}$$

ii. Reaction with alkylperoxy radical

$$NO + RO_2 \longrightarrow NO_2 + RO \qquad \text{.....(2-3)}$$

iii. Reaction with acylperoxy radical

$$NO + R\text{-}\overset{O}{\overset{\|}{C}}O_2 \longrightarrow NO_2 + R\text{-}\overset{O}{\overset{\|}{C}}\text{-}O \qquad \text{....(2-4)}$$

Hydroxyl radicals from reaction (2-2) react with carbon monoxide to form hydroperoxy radicals according to the following scheme :

$$OH + CO \longrightarrow H + CO_2 \qquad \text{.....(2-5)}$$

$$H + O_2 + M \longrightarrow HO_2 + M \qquad \text{.....(2-6)}$$

where M is a third body capable of absorbing excess vibrational energy. Acylperoxy radicals from reaction (2-4) react further with NO_2 to form peroxyacyl nitrates which are eye irritants.

Step 2. Photolysis of NO_2 -

NO_2 from reactions (2-1), (2-2), (2-3) and (2-4) will undergo photolytic reaction resulting in the formation of ozone according to

$$NO_2 \xrightarrow{h\nu} NO_2^* \longrightarrow NO + O \qquad \text{.....(2-7)}$$

$$O + O_2 \longrightarrow O_3 \qquad \text{.....(2-8)}$$

Step 3. Smog formation.

Ozone from reaction (2-8) combines with hydrocarbons present in the air to form smog following the processes represented by

$$O_3 + NO \longrightarrow NO_2 + O_2 \qquad \text{.....(2-9)}$$

$$O_3 + HC + NO_2 \longrightarrow \text{Photochemical Smog} \qquad \text{.....(2-10)}$$

In addition to these reactions, it has been suggested that nitrosoamines could be formed in the atmosphere through the reaction of NO_2 and amines. The presence of ozone has been shown to accelerate nitrosoamine formation. Inhalation of nitrosoamine has been linked to cancer in animal tests [10].

2.2.1.2 The Chemistry of NO_x Formation [21,22]

During combustion, NO_x forms via a thermal fixation of atmospheric N_2 and through conversion of fuel-bound nitrogen. Both processes are primarily responsible for the formation of NO because residence times in most combustion units are too short for the oxidation of NO to NO_2. The thermal fixation of atmospheric N_2 occurs at high temperatures (1760 ^{o}C to 1816 ^{o}C) in the presence of excess air while the conversion of fuel-bound nitrogen is relatively independent of combustion temperature. The oxidation of fuel-bound nitrogen is primarily dependent on the amount of nitrogen present in the fuel and oxygen availability.

At high temperatures and in the presence of excess air, the usually stable oxygen molecule dissociates to the unstable oxygen atom, which is highly reactive and attacks the otherwise stable nitrogen molecule to form NO via the thermal fixation mechanism. The simplified form of the overall reactions can be summarized according to the following scheme:

1. In the combustion zone where the temperatures and oxygen levels are high, nitric oxide is formed by the processes

$$N_2 + O \longrightarrow NO + N \quad \text{..... (2-11)}$$

$$N + O_2 \longrightarrow NO + O \quad \text{..... (2-12)}$$

2. Near the exit of the combustion zone, additional nitric oxide is generated but the main process is the

oxidation of NO to brownish NO_2 at lower temperature via the reactions

$$N_2 + O_2 \longrightarrow 2NO \quad \text{.....} \quad (2\text{-}13)$$

$$2NO + O_2 \longrightarrow 2NO_2 \quad \text{.....} \quad (2\text{-}14)$$

Since the residence times are so short, complete conversion of NO to NO_2 is severely limited. In addition to the discussed generation mechanism, NO_x formation from chemically bound nitrogen in the fuel is of equal importance during coal and fuel oil combustion. Recent experimental studies show that this oxidation process occurs rapidly at moderate temperatures according to [21]

$$2f\text{-}N + 2O_2 \longrightarrow 2NO + 2O \quad \text{.....} \quad (2\text{-}15)$$

where 2f-N is the fuel-bound nitrogen.

2.2.2 Sources, Regional Variations and Emission Trends of NO_x in Canada

2.2.2.1 Sources of NO_x [23]

Broadly speaking, NO_x is emitted by both natural and man-made sources. Although the natural sources are responsible for most of the NO_x emission, the major concern is over anthropogenic processes which can be subdivided for convenience into stationary and mobile sources.

The stationary and mobile sources are ultimately related to the combustion of fossil fuels. About half of the NO_x emissions in Canada come from stationary sources such as furnaces and boilers. The other half come from automobiles and other motor vehicles. Typical U.S. and Canadian emissions are summarized in Table 2-1.

TABLE 2.1

Current Nationwide Emissions of NO_x In The United States and Canada [23].

	U.S.A. 1980 (Estimated) NO_x	Canada 1979 NO_x	Total NO_x
Utilities	5.6	0.3	5.9
Industrial Boilers/ Process Heaters/ Residential/Commercial	6.4	0.5	6.9
Transportation	8.2	1.0	9.2
Other	—	0.2	0.2
Total	20.2	2.0	22.2

Unit: Millions of tonnes (1 tonne = 1.1023 tons).

As would be expected, the American contribution is far greater than the Canadian. Emissions of NO_X from U.S. sources are about ten times greater than the Canadian output (20.2 million tonnes versus 2.0 million tonnes)[23].

2.2.2.2 Regional Variations and Emission Trends in Canada [23]

Coincident with population growth, heavier resource utilization, industrial expansion, and the proliferation of the private automobile as a means of transportation, NO_X emissions have increased in Canada in all areas during the 1950 - 1978 period. In eastern Canada, NO_X emissions grew from a level of less than 0.5 million tonnes in 1955 to 1.4 million tonnes in 1977. In general, the major portion of NO_X emission increases was from thermal power plants and the transportation sector. Of great concern to eastern Canada is the level of NO_X emissions from U.S. thermal power plants located in the upper Ohio valley where a large-scale conversion of oil-fired units to coal combustion is proposed. The increased use of coal will increase NO_X emissions significantly. A substantial portion of these emissions will affect the ambient NO_X concentration levels in the eastern Canadian provinces. Figure 1-1 indicated that NO_X discharges from U.S. thermal power plants are projected to increase by about 50 percent by the year 2000 from 13.3 million tons (1980 level) to about 21.2 million tons. A similar projection for Canadian thermal power plants suggests a doubling of NO_X em-

issions from 0.3 million tonnes to 0.6 million over the next two decades [23] if the NO_x emissions are not controlled. In fact all new thermal power plants proposed for construction in Canada over the next two decades will be coal-fired. Figure 2-3 illustrates the potential NO_x emissions that have been estimated for each province. Of the eleven areas depicted, Ontario is the most serious offender. According to the report by Irwin [23], none of the provinces are embarking on a course of action to reduce NO_x emissions. Most of the NO_x emissions in Ontario come from Ontario Hydro's thermal power plants located on the St. Clair River (Lambton plant) and Lake Erie (Nanticoke plant). The emissions from the various thermal generating stations in Ontario are summarized in Figure 2-4.

Apart from stationary sources, emissions of NO_x from the transportation sector are of major concern in Canada, particularly in large urban centres. The present Canadian new-vehicle emission standard for NO_x is 3.1 grams per vehicle mile (gpm). The U.S. standard is 1.0 gpm for 1981 model passenger autombiles. It is possible that NO_x emissions from this sector could increase from 1.0 million tonnes in 1980 to 1.6 million tonnes in 2000, if no further control action is taken in this country. However, if more stringent new vehicle emission standards are adopted by 1985, Canadian NO_x emissioms in 1990 could decrease by 20 percent from 1980 levels.

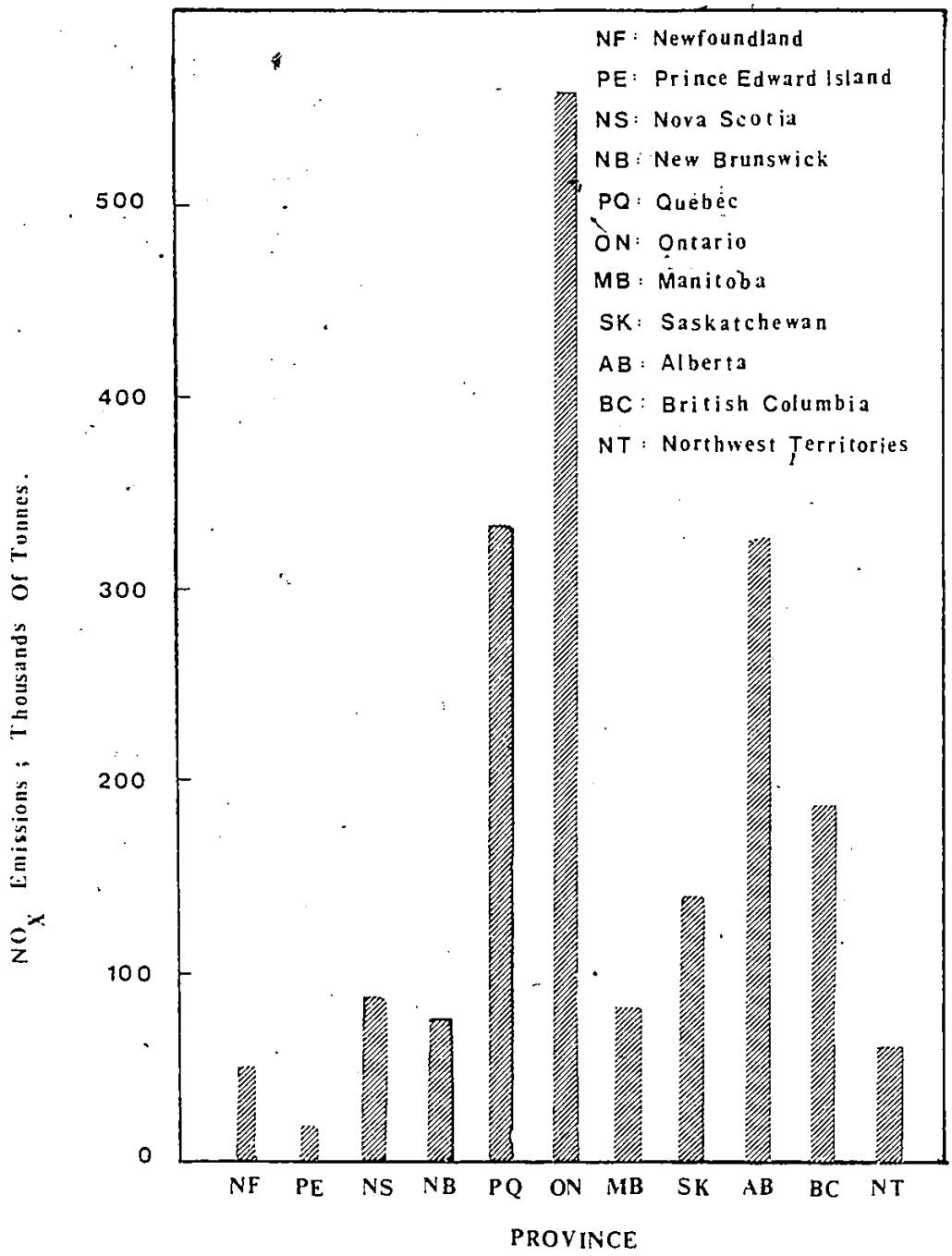

Figure 2-3 : Annual Emissions of NO_X in Canada by Province, 1976 - 1977 (23)

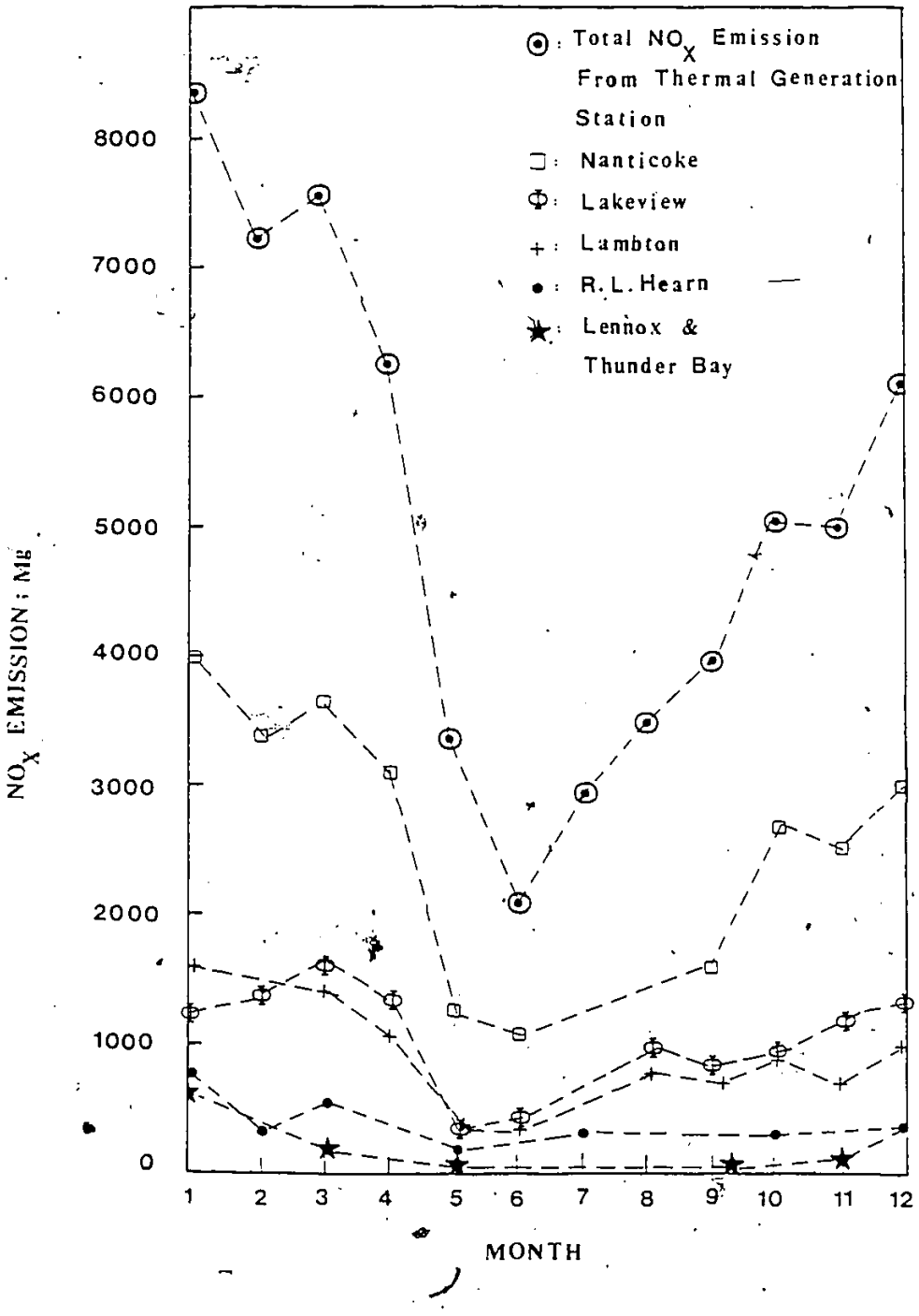

Figure 2-4 : Monthly Atmospheric NO_X Emissions from Various Thermal Generating Stations in Ontario, 1978 (24)

2.3 NO_X CONTROL TECHNOLOGY

The previous review focussed on environmental effects of NO_X, general chemistry, sources, regional variations and emission trends in Canada. Emphasis focussed on the need for controlling NO_X emission in the province of Ontario. The present section concentrates on emission control technologies. The aim is to evaluate the most promising methods available in the abatement area. Following this assessment, a potential control technology will be recommended for NO_X emissions from thermal power plants.

2.3.1 Classification of NO_X Emission Control Technologies

According to NO_X control strategies the emission of NO_X can be regulated either through suppression of NO_X formation or through flue gas treating processes (FGT). The suppression of NO_X formation can be achieved by

1. reducing peak flame temperatures and residence times in the combustion zone.
2. reducing nitrogen levels at peak flame temperature.
3. decreasing oxygen levels at peak flame temperature of the combustion process.

Such operations essentially suppress NO_X formation by hindering the thermal fixation reaction. Attempts to control NO_X emission by reducing nitrogen levels are reported to be effective [25]. By employing several combustion modification

techniques such as low excess air combustion, flue gas recirculation or staged combustion, a 30 to 50 percent reduction of NO_x emissions can be achieved in existing industrial boilers [25].

Flue gas treating processes (FGT) are commonly classified as wet or dry operations, with further distinctions based on NO_x removal alone or combined NO_x /SO_x removal. Wet processes usually utilize absorption technology while dry processes normally use catalytic decomposition or adsorption. Most dry FGT processes involve either catalytic or homogenous decomposition. Because both require high temperatures (600 - 1800 ^{o}F), they are generally integrated into the boiler or process heater ahead of the air preheater. On the other hand, wet processes are normally added on downstream of all equipment, just ahead of the stack. The major techniques available for NO_x emission control are summarized in Table 2-2.

2.3.2 Reduction of NO_x Formation

Various techniques have been proposed and used to reduce NO_x formation during combustion. Some typical approaches are listed in Table 2-2. Other methods involve

1. steam or water injection.
2. re-arrangement of burner configuration, location and spacing.
3. conversion to fluidized bed combustion.

TABLE 2.2

NO_x Control Methods [25].

Reduction of NO_x Formation	NO_x Removal From Flue Gas
1.Combustion Modification	2.Dry Process
Low excess air combustion	Selective catalytic reduction (SCR)
Flue gas recirculation	Selective noncatalytic reduction (SNR)
Staged combustion	
Low NO_x burners	
Catalytic combustion	
3.Use of Low Nitrogen Fuel	4.Wet Process
Change of fuel	Oxidation absorption
Nitrogen removal from fuel	Oxidation reduction
	Absorption reduction

As indicated earlier, the principle underlying these operations is to limit oxygen availability and to reduce peak flame temperatures in the combustion zone as a means of lowering NO_x production. It is possible to reduce NO_x formation by removing a large part of the nitrogen contained in fuels by fuel denitrogenation or to use low nitrogen fuels.

2.3.2.1 Combustion Modification

Combustion modification is the most cost-effective and energy efficient technology used to control combustion generated NO_x. It has been widely implemented on existing gas and oil fired boilers to reduce NO_x emission in the United States. However, recent commercial tryouts have shown that these techniques can limit NO_x emissions by no more than 60 percent. Table 2-3 summarizes the reduction performance of the various techniques now in use. These approaches are not effective in controlling NO_x emissions derived from coal nor applicable to high sulphur content gas and oil fuel types. Reports from recent tryouts on coal firing employing these techniques have indicated that a maximum of 40 percent reduction in NO_x emissions can be achieved using staged combustion.

A lack of efficient gas cleaning technology promotes NO_x emissions which are projected to increase by about 50 percent by the year 2000 in the United States. In Canada, the earlier review indicated that all new thermal plants

TABLE 2.3

The Performance of Various Combustion Modification Techniques [18,21,22,25,26].

Combustion Modification Techniques	Reduction in NO_x Emission (%).
a. Staged Combustion	30-50
b. Flue Gas Recirculation	20-60
c. Water or Steam Injection	40-60
d. Lower Excess Air Combustion	17-38
e. Catalytic Combustion	Not available
f. Lower NO_x Burner	65-90

proposed for construction will be coal-fired. They will be responsible for most of the projected increases in NO_x emissions. In fact, these projections emphasize the need for controlling NO_x emission in this country. Both wet and dry flue gas treating processes appear to offer some help.

2.3.2.2 Fuel Denitrogenation [18,25]

Various studies on the methods of denitrogenation have been initiated at the Industrial Environmental Research Laboratory at Research Triangle Park (U.S.A.) [18]. No commercial tryouts of the methods have yet been attempted. To date, there are limited papers describing these studies. This technology removes nitrogen from liquid fuels by mixing with hydrogen gas. Heating the mixture with a catalyst causes the nitrogen in the fuel and the hydrogen to unite to form ammonia. Current research is concentrated on the development of better catalysts and ways of reducing the deposition of carbon on the catalyst surface.

2.3.3 Flue Gas Treatment

Two types of flue gas treatment processes (dry or wet) are available as add-on technology for cleaning NO_x which is emitted from thermal power plant or related chemical-process industries. Recent commercial tryouts [11,21,25] have shown that these methods are capable of reducing NO_x emissions by 90 percent. Since the nitric oxide (NO) species represent

more than 90 percent of the NO_x emissions, removal of NO is fundamental to flue gas treating processes. The major research interests, centering around the removal of NO, are listed in Tables 2-4 and 2-5. Other flue gas treatment methods, such as dry adsorption of NO_x by solids, physical separation or electric discharge are less important due to their high costs or low capacity for removal of NO_x .

2.3.3.1 Dry Processes [11,18,21,25]

Among the dry processes, selective catalytic reduction (SCR) of NO_x with ammonia (NH_3) is the predominant technology in industrial applications. About 60 industrial plants that adopted this technique show that SCR is capable of reducing NO_x emissions by 90 percent [11]. However, despite these high NO_x removal efficiencies, the SCR method is not really applicable to coal generated flue gases due to the high particulate levels which destroy the catalyst sensitivity [21]. Other major concerns during commercial tryouts include

1. excessive NH_3 emissions.
2. NH_3 availability.
3. increased SO_3 emissions from catalytic oxidation of SO_2 .
4. deposition of ammonium bisulfate in the air preheater which causes corrosion and plugging problems.

TABLE 2.4

NO_x Flue Gas Treating Technology [25].

Dry Processes	Wet Processes
Catalytic decomposition	Absorption with liquid phase oxidation to NO_2/NO_3
Selective catalytic reduction with NH_3	Gas phase oxidation followed by absorption and liquid phase reduction.
Non-selective catalytic reduction with reducing gases.	Gas phase oxidation followed by absorption and liquid phase oxidation to NO_2 /NO_3
Adsorption by solids	Absorption with liquid reduction to NH_4 .

TABLE 2.5

NO_x /SO_x Flue Gas Treating Technology [25].

Dry Processes	Wet Processes
Selective catalytic reduction with NH_3 and adsorption of SO_2 by activated carbon.	Absorption of NO_x and SO_2 with liquid phase reduction of NO_x to N_2 by $SO_3^{=}$.
Selective catalytic reduction with NH_3 and reaction of SO_2 with copper oxide.	Absorption of NO_x and SO_2 with liquid phase oxidation to NO_3^- and $SO_4^{=}$.
Adsorption of NO_x and SO_2 by solids.	Gas phase oxidation of NO, absorption of NO_x and SO_2 with liquid phase reduction of NO_2 to N_2.
Electron beam radiation.	Gas phase oxidation of NO, absorption of NO_x and SO_2 with liquid phase oxidation of NO_x to NO_3^-.
Adsorption of NO_x /SO_x by solid.	

Newer dry processes such as electron beam radiation and adsorption by solids are in early stages of development and are less effective than the SCR method. Dry processes for simultaneous NO_x and SO_x removal are less developed. Only relatively small commercial and pilot plants have been tested with dual NO_x and SO_x removal principles employing activated carbon and copper oxide [11,25]. The evaluations of dry processes for the removal of NO_x alone and simultaneous NO_x and SO_x removal are summarized in Tables 2-6 and 2-7 respectively.

a. Dry Processes for NO_x Removal [11,18,21,25].

i. Selective Catalytic Reduction of NO_x With NH_3 (SCR).

Virtually all of the NO_x in the combustion gases is in the form of nitric oxide (NO). On the basis that NH_3 reacts selectively with NO in flue gases between 200 to 450 ^{o}C, the SCR method can be represented by the reaction

$$4NO + 4NH_3 + O_2 \xrightarrow{\text{catalyst}} 4N_2 + 6H_2O \quad \text{.....(2-16)}$$

In commercial practice an NH_3 : NO mole ratio of 1.05 : 1.0 to 1.1 : 1.0 is required to reduce NO_x emissions by 90 percent. The catalyst is a base metal such as iron, vanadium, chromium, manganese, cobalt, copper or barium deposited on a carrier of alumina, titanium dioxide or silicon dioxide. Many of these catalysts are damaged by SO_x in the flue gas. The most stable and widely used catalysts contain vanadium compounds on a titanium dicxide carrier.

TABLE 2.6

The Performance of Various Dry Processes (NO_X alone) [11, 18, 21, 25].

Dry Processes	Reduction in NO_X Emission (%)
a. Selective Catalytic Reduction of NO_X with NH_3 (SCR).	90
b. Non-Selective Catalystic Reduction	30
c. Selective Noncatalytic Reduction of NO_X (SNR).	50-60
d. Adsorption by Solids.	not available

TABLE 2.7

The Performance of Various Dry Processes (Combined NO_x/SO_x Removal) [11,21,25].

Dry Processes	Reduction in NO_x Emissions (%)
a. Selective Catalytic Reduction with NH_3 and Adsorption of SO_2 by Activated Carbon.	80-90
b. Selective Catalytic Reduction with NH_3 and Reaction of SO_2 with Copper Oxide (Shell FGT Process).	90 (SO_x) 70 (NO_x)
c. Electron Beam Radiation.	80

One major concern with SCR processes is the deposition of ammonium bisulfate below about 220 ^{o}C in the air preheater according to

$$NH_3 + SO_3 + H_2O \longrightarrow NH_4HSO_4 \quad \text{.....(2-17)}$$

which causes corrosion and plugging problems. Other potential problems are excessive NH_3 emissions, NH_3 availability and increased SO_3 emissions from catalytic oxidation of SO_2. A small amount of NO_2 present reacts with NH_3 according to

$$4NH_3 + 2NO_2 + O_2 \xrightarrow{\text{catalyst}} 3N_2 + 6H_2O \quad \text{.....(2-18)}$$

ii. Non-Selective Catalytic Reduction.

Extensive studies have emphasized the need for better NO decomposition catalysts. Maximum decomposition of NO was observed with 0.1% Pt - 3% Ni catalyst using Al_2O_3 as carrier.

iii. Selective NonCatalytic Reduction of NO_x (SNR).

NH_3 rapidly reacts with NO_x (mainly NO) around 1000 ^{o}C without catalyst to form N_2 and H_2O. The overall reaction is shown by

$$4NO + 4NH_3 + O_2 \xrightarrow{1000\,^{o}C} 4N_2 + 6H_2O \quad \text{.....(2-19)}$$

With an NH_3: NO feed ratio of 1.5 : 1.0 to 2.0 : 1.0, NO_x reductions in the range of 50 - 60 percent have been achieved in Japan on commercial boilers. Major problems are equipment corrosion, plugging due to ammoniumm sulfate and

ammonium bisulfate formation, NH_3 emissions and NH_3 usage. Advantages include low capital cost for installation, no catalyst requirement and no increased SO_3 emissions.

iv. Adsorption by Solids.

Silica gel, alumina, molecular sieves and charcoal can be used to adsorb NO_x. No commercial tryouts are reported. Major problems are low adsorption and high costs.

b. Dry Processes for Combined NO_x/SO_x Removal [11,21,25].

i. Selective Catalytic Reduction with NH_3 and Adsorption of SO_2 by Activated Carbon.

Activated carbon adsorbs SO_x and also works as an SCR catalyst, according to

$$1/2\ O_2 + SO_2 \xrightarrow{C^*} SO_3 \qquad \text{.....(2-20)}$$

Flue gas injected with NH_3 is passed through the carbon bed at about 220°C for 80 to 90 percent removal of both SO_x and NO_x represented by the schemes

$$4NH_3 + 4NO + O_2 \xrightarrow{C^*} 4N_2 + 6H_2O \qquad \text{.....(2-21)}$$

$$4NH_3 + 2NO_2 + O_2 \xrightarrow{C^*} 3N_2 + 6H_2O \qquad \text{.....(2-22)}$$

$$NH_3 + 2SO_3 + 2H_2O \xrightarrow{C^*} H_2SO_4 + NH_4HSO_4 \qquad \text{.....(2-23)}$$

Higher temperatures increase NO_x removal but decrease SO_x removal. SO_x is adsorbed by the carbon to form H_2SO_4 and NH_4HSO_4, which are removed by heating the carbon at 350 °C in an inert gas produced by incomplete combustion of fuel according to

$$2H_2SO_4 + C \xrightarrow{350\,^{\circ}C} 2SO_2 + 2H_2O + CO_2 \quad \text{.....(2-24)}$$

$$4NH_4HSO_4 + C + 2O_2 \longrightarrow 2N_2 + 10H_2O + 4SO_2 + CO_2 \quad \text{.....(2-25)}$$

$$2NH_4HSO_4 + C \longrightarrow 2NH_3 + 2SO_2 + 2H_2O + CO_2 \quad \text{.....(2-26)}$$

Concentrated SO_2 is recovered which can be used for H_2SO_4 production.

ii. Selective Catalytic Reduction with NH_3 and Reaction of SO_2 with Copper Oxide (Shell FGT Process).

This process utilizes a copper acceptor supported on stabilized alumina (Al_2O_3) which is arranged in two or more parallel passage reactors. The copper is first oxidized to copper oxide according to

$$Cu + 1/2\ O_2 \longrightarrow CuO \quad \text{.....(2-27)}$$

Copper oxide reacts with SO_2 and O_2 in the flue gas at 750°C to form copper sulfate by the process

$$SO_2 + 1/2\ O_2 + CuO \longrightarrow CuSO_4 \quad \text{.....(2-28)}$$

Both Cu and $CuSO_4$ work as SCR catalysts for selective reduction of NO_x by NH_3 at about 400 °C according to

$$4NO + 4NH_3 + O_2 \xrightarrow{CuO\ ;\ CuSO_4} 4N_2 + 6H_2O \quad \text{....(2-29)}$$

$$2NO_2 + 4NH_3 + O_2 \xrightarrow{Cu\ ;\ CuSO_4} 3N_2 + 6H_2O \quad \text{....(2-30)}$$

The reactor is regenerated when saturated with $CuSO_4$. Hydrogen is used to reduce copper sulfate to copper by the reaction

$$CuSO_4 + 2H_2 \longrightarrow Cu + SO_2 + 2H_2O \quad \text{.....(2-31)}$$

and then purged with steam to remove combustible gases. Concentrated SO_2 is recovered for producing sulfuric acid.

iii. Electron Beam Radiation.

Flue gas at about 100°C is mixed with NH_3 and exposed to electron beam radiation. The prime advantage is that only electricity is needed to lower emissions. However, electrostatic precipitators are involved in the removal of particulate matter. No ccmmercial tryouts are reported.

2.3.3.2 Wet Processes [21,25]

Previous discussions showed that neither combustion modifications nor SCR methods are effective or applicable for controlling NO_x emissions generated from coal-fired thermal generating stations. However, wet technology designed for simultaneous NO_x/SO_x removal is especially well suited for high sulfur oil or coal firing operations. A major problem associated with this method is the relatively low solubility of NO in absorbing solutions as compared to NO_2. In order to obtain high levels of NO_x removal, prior oxidation of NO to NO_2 is necessary in either the liquid or the gas phases.

Typical liquid and gas phase oxidants such as potassium permanganate, hydrogen peroxide, sodium chlorite, ozone and chlorine dioxide have some commercial applications which are summarized in Tables 2-8 and 2-9. Two of the more promising wet technologies are absorption reduction and oxidation absorption reduction. Small scale commercial tryouts show that these processes can remove 80-90 percent NO_x with over 95 percent SO_2 collection [25]. However, a major drawback of this method is due to high capital costs and process complexity. To date there are only 13 commercial applications of wet processes which are all in Japan. Table 1-3 describes these Japanese applications.

a. Wet Processes for NO_x Removal [21,27,28,29,30,31,32]

i. Absorption with Liquid Phase Oxidation to NO_2/NO_3

The emitted flue gas, mainly NO, is oxidized either with potassium permanganate, hydrogen peroxide or sodium chlorite before being scrubbed with sodium hydroxide solution. However, these processes are less important than SCR or SNR methods for NO_x removal. No commercial tryouts are reported.

ii. Gas Phase Oxidation Followed by Absorption and Liquid Phase Reduction.

Gas phase oxidants such as O_3 or ClO_2 are used to oxidize insoluble NO to the more soluble nitrogen dioxide.

TABLE 2.8

The Performance of Various Wet Processes (NO_x alone) [21,27,28,29,30,31,32].

Wet Processes	Reduction in NO_x Emission (%)
a. Absorption with Liquid Phase Oxidation to NO_2/NO_3.	
1. Potassium Permanganate	70-80
2. Hydrogen Peroxide	not available
3. Concentrated Nitric Acid (60-80%)	not available
4. Sodium Chlorite	40-80
b. Gas Phase Oxidation Followed by Absorption and Liquid Phase Reduction.	
1. Sulfite Solution	85-90
c. Gas Phase Oxidation Followed by Absorption and Liquid Phase Oxidation to NO_2/NO_3	
1. Sodium Chlorite Solution	90
d. Absorption with Liquid Phase Reduction	
1. Sodium Sulfite	90

TABLE 2.9

The Performance of Various Wet Processes (Combined NO_x/SO_x Removal)[11,21,25,27].

Wet Processes	Reduction in NO_x Emission (%)
a. Absorption of NO_x and SO_2 with Liquid Phase Reduction of NO_x to N_2 by SO_3^{-2}.	
Na_2CO_3	90
b. Absorption of NO_x and SO_2 with Liquid Phase Oxidation to NO_3^- and SO_4^{-2}	
Alkali Permanganate	90
c. Gas Phase Oxidation of NO, Absorption of NO_x and SO_2 with Liquid Phase Reduction of NO_2 to N_2.	
$CaSO_3$	90 (NO_x)
$CaCO_3$	95 (SO_x)
d. Gas Phase Oxidation of NO. Absorption of NO_x and SO_2 with Liquid Phase Oxidation of NO_x to NO_3^-.	
Sodium chlorite	90

Addition of ferrous ethylenediaminetetraacetic acid (Fe.EDTA) as catalyst is needed to aid absorption of NO. The NO_x in solution is then reduced by SO_3^{-2} ion to form N_2. Processes can be modified to provide both NO_x and SO_x removal. Most are relatively insensitive to inlet flue gas compositions.

iii. Gas Phase Oxidation Followed by Absorption and Liquid Phase Oxidation to NO_2 /NO_3

Chlorine dioxide oxidizes NO to NO_2 which is scrubbed with $NaClO_2$ solution.

iv. Absorption with Liquid Phase Reduction.

Sodium sulfite from desulfurization processes is used to scrub NO_x which is further reduced to N_2 after absorption. Large flow rates and excess O_2 hinder reduction.

b. Wet Processes for Combined NO_x/SO_x Removal [11,21, 25,27].

i. Absorption of NO and SO_2 with Liquid Phase Reduction of NO to N_2 by SO_3^{-2}.

This absorption reduction process avoids gas phase oxidation by using the ferrous chelating compound Fe.EDTA in alkaline sodium carbonate solution tc improve the NO absorption according to

$$NO + Fe.EDTA \longrightarrow Fe.EDTA.NO \quad \ldots\ldots (2\text{-}32)$$

SO_x is simultaneously absorbed as sodium sulfite and reacts with the NO complex to yield nitrogen, a regenerated chelating compound and sodium sulfate as illustrated by

$$Na_2CO_3 + SO_2 \longrightarrow Na_2SO_3 + CO_2 \quad \text{------(2-33)}$$

$$Na_2SO_3 + Fe.EDTA.NO \longrightarrow Fe.EDTA + Na_2SO_4 + 1/2\ N_2 \quad \text{-------(2-34)}$$

These processes are less desirable than dry processes because they involve considerable equipment and complex chemistry. No commercial applications are reported.

ii. Absorption of NO_x and SO_2 with Liquid Phase Oxidation to NO_3^- and SO_4^{-2}.

NO_x and SO_2 are absorbed and oxidized with alkali permanganate to form alkali nitrate and sulfate. Manganese dioxide precipitate is reduced for reuse. Nitrate is used for fertilizer. Alkali KOH and permanganate production are expensive.

iii. Gas Phase Oxidation of NO, Absorption of NO_x and SO_2 with Liquid Phase Reduction of NO_2 to N_2.

A gas phase oxidizing agent, (ozone or chlorine dioxide) is injected into the flue gas to convert NO to NO_2 prior to absorption by the following reactions

$$NO + O_3 \longrightarrow NO_2 + O_2 \quad \text{-----(2-35)}$$

$$2NO + ClO_2 + H_2O \longrightarrow NO_2 + HNO_3 + HCl \quad \text{-----(2-36)}$$

NO_2 is then absorbed into an aqueous solution containing calcium sulfite and carbonate while SO_x is absorbed and forms the sulfite or bisulfite ion in the scrubbing solution according to

$$2NO_2 + CaSO_3 + CaCO_3 + 2H_2O \longrightarrow Ca(NO_2)_2 + CaSO_4 \cdot 2H_2O + CO_2 \quad \text{.....(2-37)}$$

$$CaSO_3 + SO_2 + H_2O \longrightarrow Ca(HSO_3)_2 \quad \text{.....(2-38)}$$

Bisulfite ions are then partially oxidized to sulfate during reduction of the NO_2 by way of

$$Ca(HSO_3)_2 + Ca(NO_2)_2 + 2H_2O \longrightarrow N_2 + 2CaSO_4 \cdot 2H_2O \quad \text{.....(2-39)}$$

Problems include the complex chemistry and extensive equipment requirements.

iv. Gas Phase Oxidation of NO. Absorption of NO_x and SO_x with Liquid Phase Oxidation of NO_x to NO_3^-

A gas phase oxidant such as O_3 or ClO_2 is used to oxidize NO to NO_2. The produced NO_2 is then scrubbed by sodium chlorite.

2.4 CONCLUSION

According to this review, most of the emissions of NO_x in Canada are from stationary combustion and transportation sectors. Of the eleven major Canadian areas, Ontario is responsible for most of the toxic oxides of nitrogen. About half of the Ontario NO_x emissions come from stationary combustion facilities which represent Ontario Hydro thermal power plants. To date, none of the provinces have embarked on a course of action to reduce NO_x emissions. It has been pointed out that all new thermal power plants proposed for construction over the next two decades will be coal-fired.

The hazards of the toxic oxides of nitrogen to human health, vegetation and the environment are well documented. This review indicated that many provinces experience an acid rain problem which is due mainly to the uncontrolled NO_x and SO_x emissions in this country. A projection of NO_x production shows that thermal power plants will double NO_x emissions over the next two decades if no controls are instituted. Concern about the health effects of NO_x has led some affected jurisdictions, mostly in the United States and Japan but not in Canada, to initiate some regulatory activities. This review emphasises the need for controlling NO_x emissions in this country especially in the province of Ontario. The most effective way of reducing NO_x levels is to limit emission from coal-fired thermal power plants.

Various technologies have been developed for NO_x emission control purposes. These include combustion modifications and flue gas treatment processes. Recent commercial tryouts on combustion modifications have shown that these techniques are not effective nor applicable to the reduction of NO_x emissions generated from coal- fired plants. Nevertheless the combustion modification techniques are the most cost effective methods among the existing control technologies. Although staged combustion has a limitation of reducing NO_x emissions by only 40 percent when applied to coal-fired generation of NO_x, it should be used to reduce the concentration of NO_x as low as possible prior to the flue gas treatment.

For further reduction of NO_x emission from coal firing, flue gas treatment processes appear to provide a solution. However, the most widely utilized flue gas technology - selective catalytic reduction (SCR) with NH_3 is not useful for handling coal derived NO_x emission mainly because of SO_x and particulate poisoning problems. In general the dry processes are most effective for the cleaner flue gases resulting from oil and gas firing. Other dry processes, such as electron beam radiation and adsorption by solids, are in early stages of development and are not yet promising.

Due to higher capital costs, wet process technology is less favorable than dry processes for commercial applica-

tions. However, the wet technology appears to be especially well suited for simultaneous removal of NO_X and SO_X generated by high sulphur oil and coal-fired thermal power plants. Figure 2-5 illustrates the relationship of SO_X and NO_X concentrations in flue gases to suitable processes for treatment. The cost of these methods are summarized in Tables 2-10 and 2-11.

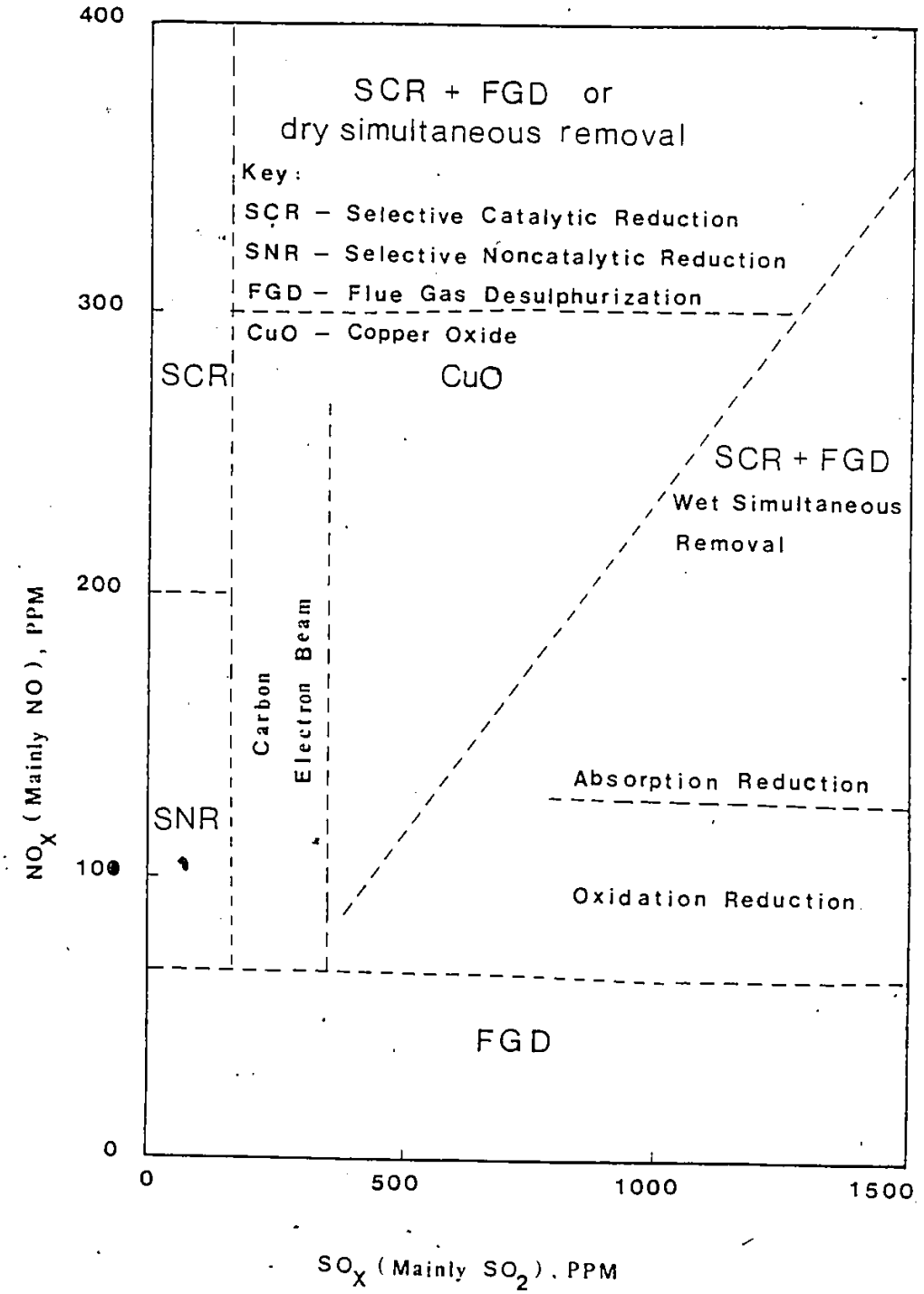

Figure 2-5 : Relationships of SO_x and NO_x Concentrations in Flue Gas to Suitable Processes for Treatment (25)

TABLE 2.10

Cost of NO_x and NO_x/SO_x Control Systems in the U.S.[25]

Process Type	Pollutant Removed	Capital Cost ($/kW)	Revenue Requirement (mills/kWh)
1. Selective Catalytic Reduction (SCR)	NO_x Particulate	64	3.4
2. Flue Gas Desulfurization (FGD)	SO_2	101	4.2
3. SCR +FGD	NO_x, SO_2, Particulate	165	7.6
4. Dry, Simultaneous (UOP-Shell)	NO_x, SO_2, Particulate	160	7.3
5. Wet, Simultaneous	NO_x, SO_2, Particulate		
Moretana (ClO_2)		205	12.2
Asahi (EDTA)		233	12.6
IHI (Ozone)		482	19.8

Basis for the Estimate:

Particulate Control System	ESP for dry systems; wet scrubber for wet simultaneous systems
FGD System	Limestone
SO_2 Removal Efficiency	90%
NO_x Removal Efficiency	90%
Particulate Removal Efficiency	99.5%
Boiler Size	500 MW, new
Fuel	coal
Heating value	24.4 MJ/kg (10,500 Btu/lb)
Sulfur content	3.5%
Ash content	16%
Operation	7000 hr/yr
Capital Investment	mid-1979
Annual Revenue Requirement	mid-1980

TABLE 2.11

Cost of NO_x and NO_x/SO_x Control Systems In Japan [25].

Process Type	Pollutant Removed	Capital Cost ¥/kW	Capital Cost $/kW	Operating Costs ¥/kWh	Operating Costs mills/kWh
1. Selective Catalytic Reduction (SCR)	NO_x	2800	15.5	0.3	1.6
2. Flue Gas Desulfurization (FGD)	SO_2	14000	77.8	1.2	6.7
3. SCR + FGD	NO_x & SO_2	18500	102.8	1.5	8.3
4. Simultaneous NO_x/SO_x (dry and wet)	NO_x & SO_2	20000	111.1	1.7	9.4

Basis for estimate:

Plant Size	300 MW, new	Maintenance	3% of investment cost
Fuel	oil	Insurance	2% of investment
NO_x Concentration	200 PPM	Overhead	5% of Investment cost
SO_x Concentration	1500 PPM	Catalyst Life	2 years
Particulate Concentration	200 mg/Nm	Annual Operation.	8,000 hours
Temperature	380 °C	Ammonia	¥ 80/kg
NO_x Removal Efficiency	80%	Power	¥ 12/kWh
SO_x Removal Efficiency	90%	Steam	¥ 2/kg
Depreciation	7 years	Kerosene	¥ 32/kg
Interest Per Year	10%	Monetary Conversion Rate	¥ 180/$

REFERENCES

1. Fujiwara T., Acute Effects of Combination of SO_2, NO_2 and Ozone on Some Plants. Denryokn Chuo Kenkyusho Hokokn, pp.21, Japan, (1976).

2. Ashenden T.W. and Mansfield T.A., Extreme Pollution Sensitivity of Grasses When SO_2 and NO_2 Are Present in The Atmosphere Together. Nature, 273, pp.142-143, London, (1978).

3. Matushima J., Sensitivities of Plants to Ethylene and NO_2 and the Characteristic Changes in Fine Structure of the Cell. Proc. Int. Clean Air Congr., 4, pp.112-115, (1977).

4. Troiano J.J. and Leone I.A., Changes in Growth Rate and Nitrogen Content of Tomato Plants After Exposure to NO_2 Phyropathology (Ecology and Epidemiology), 67, pp.1130-1133, (1977).

5. Durmishidze S.V. and Nutsubidze N.N., Absorption of NO_2 by Plant Leaves. Biosfera Chel. Mater. Vses. Simp., Edited by Kovda V.A., Published in Russ., (1975).

6. Popov V.A., Effect of NH_3 and NO_2 on Pigments of Tree Plastids. Russ.,Doc.No.NINITI 3278-74, (1974).

7. Capron T.M. and Mansfield T.A., Inhibition of Net Photosynthesis in Tomato in Air Polluted with NO and NO_2, Jour. Expt. Bot., 27, pp.1181-1186, (1976).

8. Li-Yung Hou, Clyde Hall A. and Abbas S., Influence of CO_2 on the Effects of SO_2 and NO_2 on Alfalfa. Environ. Poll., 12, pp.8-16, (1977).

9. Globe and Mail, Ontario Enters U.S. Pollution Case. (March 13, 1981).

10. Osie F.V., Final Report on Acidic Precipitation, Abatement of Emissions from The International Nickel Company Operations at Sudbury, Pollution Control in the Pulp and Paper Industry, and Pollution Abatement at the Reed Paper Mill in Dryden. Legislature of the Province of Ontario Standing Committee on Resources Development, Ontario Gov't Doc's, (October, 1979).

11. Ando J., Japan Reduces SO_x and NO_x - Hydrocarbon Processing, pp. 64k-64v, (August, 1979).

12. Innes W.B., Effect of Nitric Oxide Emissions on Photochemical Smog. Purad Inc. Publication, 724 Kilbourne Drive, Upland, C.A., 91786, (1978).

13. Pattle R.E. and Down P., Lung Surfactant and Its Possible Reaction to Air Pollution. Arch. Environ. Health, 14(1), pp. 70-76, (January, 1967).

14. Richters Valda, Influence of 0.5 ppm NO_2 Exposure of Mice on Maciophage Congregation in the Lungs. In Vitrs, 14(5), pp. 458-464, (1978).

15. Kim J.C.S., Cell Renewal Response to NO_2 Gas Effects in Repeated Intermittent Exposures in Hamsters. Environmental Pollution, 15(4), pp. 289-302, (1978).

16. Folinskee J.J., Effect of 0.62 ppm NO_2 on Cardiopulmonary Function in Young Male Non-Smokers, Environ. Res., 15(2), pp. 199-205, (1978).

17. Mazruik A.N. and Evans D.G., Metabolic and Immunologic Activities of Alveolar Macrophages, Arch. Environ. Health, 14(1), pp. 92-96, (January, 1967).

18. Stephen J. Gage, Research Summary, Controlling Nitrogen Oxides. EPA-600/8-80-004, EPA, USEPA Cincinnati, OH 45268, (February 1980).

19. Doyle J.J., Sulfur Dioxide Role in Eye Irritation. Arch. Environ. Health, 3, pp. 657-667, (December, 1961).

20. Corbett W.E., Assessment of the Need for NO_x Flue Gas Treatment Technology, EPA-600/7-78-215, U.S. Environmental Protection Agency, Washington, DC 20460, (November, 1978).

21. Yaverbaum L.H., Nitrogen Oxides Control and Removal, Recent Developments. pp. 5-7, Noyes Data Corporation, Park Ridge, New Jersey, U.S.A., (1979).

22. Coe W.W., Combustion: Efficiency Vs. NO_x - Hydrocarbon Processing, pp. 130-134, (May, 1980).

23. Ronald Irwin, M.P., Still Waters, Report of the Sub-Committee on Acid Rain of the Standing Committee on Fisheries and Forestry. Cat. No. XC 29-321/2-01E, Minister of Supply and Services Canada, Ottawa, Ontario, (1981).

24. Reeves J.A., Estimates of Atmospheric Emissions From Fossil-Fuel-Fired Thermal Generating Stations, 1978. CTS-07120-1, Environmental Protection Central Thermal Services, Ontario Hydro, Ontario; (February, 1979).

25. Siddiqi A.A. and Tenini J.W., NO_x Controls in Review. Hydrocarbon Processing, pp.115-124, (October, 1981).

26. England G.C., Control of NO_x Emissions. Hydrocarbon Processing, pp. 167-171, (January, 1980).

27. Siddiqi A.Z. and Tenini J.W., Control NO_x Emissions from Fixed Fireboxes. Hydrocarbon Processing, pp.94-97, (October, 1976).

28. Teramoto M., Hiramine S., Shimada Y., Sugimoto Y. and Teranishi H., Absorption of Dilute Nitric Monoxide in Aqueous Solutions of Fe(II)-EDTA and Mixed Solutions of Fe(II)-EDTA and Na_2SO_3. Journal of Chemical Engineering of Japan, 11, No.6, pp.450-457, (1978).

29. Sada E. and Kumazawa H., Absorption of NO in Aqueous Solutions of Fe(III)-EDTA Chelate and Aqueous Slurries of MgSO with Fe(III)-EDTA Chelate. Industrial Engineering Chemistry Process Design Development, 20, No.1, pp.46-49, (1981).

30. Lefers J.B., de Boks F.C., Bleek van den C.M., and Berg van den P.J., The Oxidation and Absorption of Nitrogen Oxides in Nitric Acid in Relation to the Tail Gas Problem of Nitric Acid Plants. Chemical Engineering Science, 35, pp.145-153, (1980).

31. Baveja K.K., Subba Rao D., and Sarkar M.K., Kinetics of Absorption of Nitric Oxide in Hydrogen Peroxide Solutions. Journal of Chemical Engineering of Japan, 12, No.4, pp.322-325, (1979).

32. Sada E. and Kumazawa H., Absorption of NO in Aqueous Mixed Solutions of $NaClO_2$ and NaOH. Chemical Engineering Science, 33, pp.315-318, (1978).

III. ABSORPTION THEORY REVIEW

The previous literature survey indicated that the simultaneous removal of NO_x/SO_x from flue gases by chemical absorption with aqueous solutions is well suited for high sulphur dioxide or high particulate emission processes. It is worthwhile at this point to review the basic mechanisms of absorption before proceeding to the model derivation in the next chapter.

3.1 THE MECHANISMS OF ABSORPTION

Two theories have been proposed for describing the mechanisms of gas-liquid absorption. These are the two-film [1] and penetration models [2]. On the basis of these two theories, different expressions can be derived for the prediction of absorption rates. The difference between the two approaches lies in the parameter which is used to account for the hydrodynamic properties of the system.

In the two-film theory, the hydrodynamic properties of the system are discussed in terms of a stagnant film thickness, δ, which assumes, depending on the geometry, liquid agitation and physical properties. According to the penetration theory, the liquid exposure time, θ, is used to ac-

count for the hydrodynamic properties of the system. The choice of one of the two theories is mainly a matter of convenience, particularly when the differences in the diffusivities of the solutes and reactants are insignificant. In many cases, the differences between predictions made on the basis of these two theories will be less than the uncertainties in the values of the physical quantities used in the calculation [3]. Thus these two theories can be regarded as interchangeable for many purposes, with selection of one being merely a matter of convenience in handling the mathematical problem. In general, computations relating to the film theory are simpler since they involve ordinary rather than partial differential equations.

3.1.1 The Two-Film Theory [4,5]

The mechanism of the absorption process for a flue gas-liquid reaction can be pictured in terms of component A (NO, NO_2, SO_2) in the gas phase reacting with a component B (NaOH, $NaClO_2$) in the liquid. Component A in the bulk flue gas is first brought to the vicinity of the phase boundary by convection currents. In the vicinity of the phase boundary, it is assumed that the convection currents die out. As a result, the creation of a thin film is postulated. Component A then must diffuse through the thin film by molecular diffusion to reach the gas-liquid interface.

At the interface, it is assumed that the flue gas component A immeasurably rapidly establishes equilibrium with the liquid and component A dissolves physically to an extent depending on its solubility in the liquid. The dissolved component A is transferred from the interface into the liquid whereas component B diffuses from the bulk liquid toward the phase boundary through a thin liquid film. Finally, the reaction product is transported out of the reaction zone. However, if the reaction rate is immeasurably high, the reaction zone becomes infinitely thin and frequently coincides with the interface. According to this theory, the rate of absorption of component A is controlled by the rate of diffusion through the two films where all the resistance is assumed to lie.

The foregoing mechanism can be described by a mathematical expression based on Fick's law which states that the rate of transfer by difussion is proportional to the concentration gradient and to the area of interface over which the diffusion is occurring.

Figure 3.1 and Figure 3.2 show the concentration profiles in the gas and liquid phases for the case of pure physical absorption and for absorption combined with chemical reaction respectively.

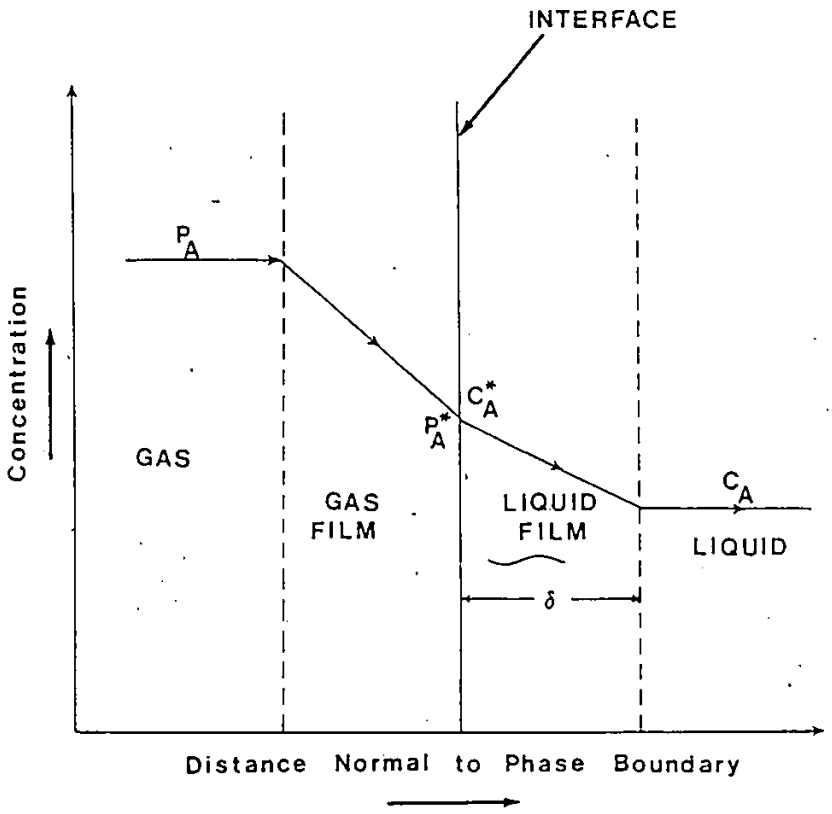

Figure 3-1 : Physical Absorption

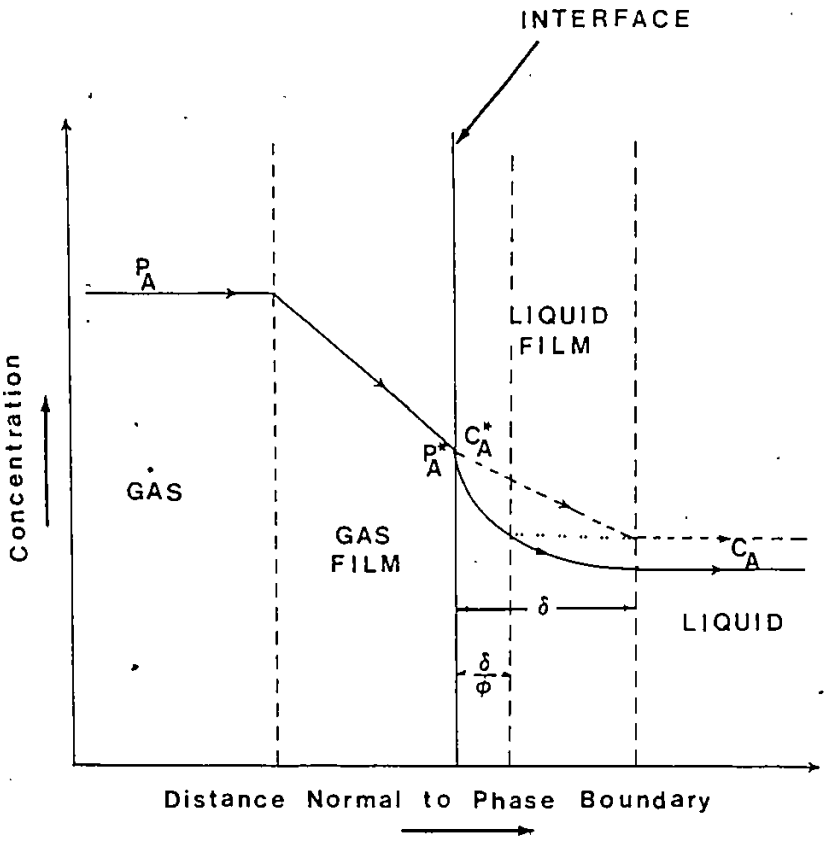

Figure 3-2 : Chemical Absorption

3.1.1.1 Physical Absorption

In Figure 3.1, the driving force in the gas phase is equal to $(P_A - P_A^*)$. The rate of mass transfer of component A through the film is given by

$$(N_A)_G = k_G (P_A - P_A^*) \qquad \text{-------(3-1)}$$

where $(N_A)_G$ = rate of mass transfer of component A through the gas film, [Kmole.m^{-2}.s^{-1}]

k_G = gas side mass transfer coefficient, [Kmole.m^{-2}.s^{-1}.atm^{-1}]

P_A = partial pressure of component A in bulk gas, [atm]

P_A^* = partial pressure of component A at interface, [atm]

whereas in the liquid phase, the physical transport of A from the interface without a chemical reaction is represented by

$$(N_A)_L = \frac{D_{AL}}{\delta}(C_A^* - C_A) \qquad \text{--------(3-2)}$$

where $(N_A)_L$ = rate of absorption of component A in the liquid phase, [Kmole.m^{-2}.s^{-1}]

D_{AL} = liquid phase molecular diffusivity of gaseous component A, [m^2.s^{-1}]

δ = effective liquid film thickness, [m]

C_A = bulk concentration of the absorbing gaseous component A in liquid absorbent, [Kmole.m^{-3}]

C_A^* = interfacial concentration of the absorbing gaseous component A in liquid absorbent, [Kmole.m^{-3}].

Since it is impossible to measure the film thickness, δ, the liquid side mass transfer coefficient k_L is defined by

$$k_L = \frac{D_{AL}}{\delta} \qquad \text{------(3-3)}$$

so that Equation (3-2) can be rewritten as

$$(N_A)_L = k_L (C_A^* - C_A) \qquad \text{------(3-4)}$$

where k_L = liquid side mass transfer coefficient, [m.s^{-1}]. In a steady state process of absorption, the rate of physical absorption is given by

$$(N_A)_{Phy} = k_G (P_A - P_A^*) = k_{L_{Phy}} (C_A^* - C_A) \qquad \text{------(3-5)}$$

where $(N_A)_{Phy}$ = physical absorption rate of component A, [Kmole.m^{-2}.s^{-1}]

3.1.1.2 Chemical Absorption

In Figure 3.2, the concentration profile across the original liquid film thickness, δ, is represented by a curve when a chemical reaction accelerates the elimination of A from the interface. For the same rate of physical absorption, the dashed line represents the concentration profile for component A being removed by diffusion alone. There-

fore, for the chemical absorption case, the effective diffusion path must be Ø times smaller than the total liquid film thickness, δ, postulated for the original rate of absorption determined by a physical absorption. From this, it follows that

$$(N_A)_{Chem} = \frac{D_{AL}}{\frac{\delta}{\emptyset}} (C_A^* - C_A) = k_{L_{Chem}} (C_A^* - C_A) \quad \text{------(3-6)}$$

where Ø, representing the degree of acceleration of the absorption due to chemical reaction, is generally referred to as the enhancement factor which may be defined as

$$\emptyset = \frac{(k_L)_{Chem}}{(k_L)_{Phy}} \quad \text{------(3-7)}$$

3.1.2 The Penetration Theory [6,7]

In the penetration theory, it is assumed that the liquid absorbent flows down over a piece of absorber packing in laminar plug flow. Component A in the gas phase is brought to the interface by convection currents. At the interface, it is assumed that the gas component A immediately establishes equilibrium with the liquid surface. Absorption takes place for a given exposure time interval by molecular diffusion and accumulation within a slug of liquid as it flows down the packing. The liquid is completely and instantaneously mixed as it flows down from one piece of packing to the next. This means that each slug begins each contact-time interval with flat concentration profiles for all liquid

components. To reduce the formulation difficulty, the contact-time between successives mixing points is so short that component A never penetrates deeply enough to approach the wall of the packing material. Thus, the depth of the liquid element is assumed to be infinite for calculation purposes.

Application of the theory to the formulation of the absorption problem will often result in non linear partial differential equation. In applying Fick's second law of diffusion (Equation 3-8) together with the boundary conditions 3-9 which are given by the theory, we obtain various models for predicting the rate of absorption.

$$D_{AL} \frac{\partial^2 C_A}{\partial x^2} = \frac{\partial C_A}{\partial t} + r \qquad \text{.....(3-8)}$$

$$\left.\begin{array}{lll} t = 0 & 0 < x < \infty & C_A = C_A \\ t > 0 & x = 0 & C_A = C_A^* \\ t > 0 & x = \infty & C_A = C_A \end{array}\right\} \qquad \text{.....(3-9)}$$

where D_{AL} = liquid phase molecular diffusivity of gaseous component A, $[m^2.s^{-1}]$

C_A = bulk concentration of the absorbing gaseous component A in liquid absorbent, $[Kmole.m^{-3}]$

C_A^* = interfacial concentration of component A in liquid absorbent, $[Kmole.m^{-3}]$

r = local rate of reaction, $[Kmole.m^{-3}.s^{-1}]$

x = distance beneath liquid surface, [m]

t = contact-time, [s]

For physical absorption with the rate of reaction, r, equal to zero, Equation 3-8 can be solved analytically with conditions 3-9, to give [3,7]

$$(N_A)_{Phy} = \sqrt{\left(\frac{D_{AL}}{\pi t}\right)}\ (C_A^* - C_A) \qquad \text{.....(3-10)}$$

where the liquid phase mass transfer coefficient is defined as

$$k_L = \sqrt{\left(\frac{D_{AL}}{\pi t}\right)} \qquad \text{.....(3-11)}$$

For chemical absorption, a known or an assumed kinetic rate form [6, 8], is neccessary to solve Equation 3-8. This partial differential equation will be normally very complicated or impossible to solve analytically. Therefore, the finite difference method is recommended [6] for solving the problem by computer.

It is interesting to note that the penetration theory predicts that k_L, the liquid film mass transfer coefficient (Equation 3-11), should be proportional to $D_{AL}^{\frac{1}{2}}$ whereas the two-film theory predicts that k_L is proportional to D_{AL} (Equation 3-3). The former relationship approximates what was found from experiments on packed columns, as reported by Sherwood and Pigford [9].

REFERENCES

1. Whiteman W.G., Two-Film Theory of Absorption. Chem. Met. Eng. 29, pp.147, (1923).

2. Higbie R., The Rate of Absorption of Pure Gas into a Still Liquid During Short Periods of Exposure. Trans. Am. Inst. Chem. Eng., 31, pp.365, (1935).

3. Danckwerts P.V., Gas-Liquid Reactions. pp.6, 33, 104, McGraw Hill Book Co.,New York, (1970).

4. Coulson J.M.,and Richardson J.F., Chemical Engineering. 2nd Ed., Vol.2, pp.433-434, 436-439, Pergamon Press, Great Britian, (1976).

5. Van Krevelen D.W., and Hoftyzer P.J., Graphical Design of Gas-Liquid Reactors. Chemical Engineering, 2, No.2, pp.145-156, (1953).

6. Brian P.L.T., Hurley J.F., and Hasseltine E.H., Penetration Theory for Gas Absorption Accompanied by a Second Order Chemical Reaction. A.I.Ch.E. Journal, 7, pp.226-231, (June, 1961).

7. Coulson J.M.,and Richardson J.F., Chemical Engineering. 3rd Ed., vol.1, pp.281, 285-289, Pergamon Press, Great Britain, (1977).

8. Barrets G.F., An Approximate Solution to The Simulataneous Chemical Absorption of Two Gases. One Gas Reacts Instantaneously. The Chemical Engineering Journal, 24, pp.81-87, (1982).

9. Sherwood T.K., and Pigford R.L., Absorption and Extraction. pp.289, McGraw Hill Book Co., New York, (1952).

IV. DERIVATION OF ABSORPTION MODELS FOR PACKED COLUMNS

Various theories [1,2,3,4,5,6], have been proposed for the prediction of absorption rates and evaluation of mass transfer coefficients. However, none of these theoretical models have proved to be adequate for predicting absorption rates in packed columns. Consequently empirical correlations are recommended [7,8,9, 10,11,12,13].

This chapter describes the development of a new absorption model that will be useful for predicting the rate of absorption in packed columns by accounting for the semi-stagnant liquid pockets depicted by the liquid residence time distribution function. As suggested by Baldi and Sicardi [4,5], trickle flow conditions are assumed to prevail in the column.

4.1 NATURE OF TRICKLING FLOW [4,5]

The nature of trickling flow is so complicated that it is very difficult to model or describe it well from a physical point of view. However, Baldi and Sicardi [4,5] suggested a simplified physical picture: According to them there are a number of random rivulets which flow separately for a certain height of packing to form new rivulets or 'die' into a

film or a pocket, from which other rivulets are again formed. The rivulets are likely to be responsible for the main liquid flow rate. A small fraction of the liquid flows as films with different velocities. The zones with lower liquid velocities can represent the 'dead' zones which can be active or inactive to mass transfer. During physical absorption, these 'dead' zones most probably will be saturated by the absorbing gas and hence ineffective to mass transfer. However, when the absorption is accompanied by chemical reaction, these zones will still be effective.

According to Michell [14], the trickle flow assumption can be justified if the Peclet number falls in the range

$$0.2 < Pe < 1.2 \qquad \text{.....(4-1)}$$

The true upper Peclet limit for trickle flow is probably 2 [15].

4.2 DERIVATION OF ABSORPTION MODELS FOR PACKED COLUMNS

In this section, we derive the mass transfer model for a packed column under countercurrent flows with the gaseous component 'A' fed to the bottom of column. The problem to be considered is that of a gaseous component 'A' travelling up a column and dissolving into the liquid phase according to Equation 4-2

$$A_G \rightleftharpoons A_L \qquad \text{.....(4-2)}$$

Subsequent irreversible reaction with component B occurs as illustrated by Equation 4-3

$$\mathcal{F}_A A_L + \mathcal{F}_B B_L \longrightarrow \text{Product} \qquad \text{.....(4-3)}$$

where component B is a nonvolatile solute which has been dissolved in the liquid phase prior to its introduction into the packed column and $\mathcal{F}_A$ and $\mathcal{F}_B$ are stoichicmetric coefficients.

Assuming the whole column is divided into a series of stages of equal height such that [4]

$$\Delta Z = \frac{Z}{n} \qquad \text{.....(4-4)}$$

where Z = total height of packing, [m]

n = number of stages, dimensionless

it is further assumed that the liquid flow pattern in each of these stages will approximate trickle flow conditions. According to the physical picture of trickle flow, the liquid will percolate via a number of segregated streams with different residence times. Let us define these stream residence times by [4]

$$t_i = \frac{S \Delta Z \delta h_i}{\delta q_i} \qquad \text{.....(4-5)}$$

where t_i = stream residence time, [s]

S = column cross sectional area, [m^2]

ΔZ = height of a stage, [m]

δh_i = liquid hold-up for a stream i, [$m^3 . m^{-3}$]

δq_i = volumetric flowrate for a stream i, [$m^3 . s^{-1}$]

We also assume the liquid flows in each stream as piston type. If δq_i is the flow rate of stream i, then $(S\Delta Z \delta h_i)$ represents the volume occupied by this stream. The distribution of these times for the stream of liquid absorbent leaving the column may be defined as [16]

$$\sum_i^{\infty}\left(\frac{q_i}{Q}\right) = \int_0^{\infty} E(t)dt = 1 \qquad \text{.....(4-6)}$$

and the mean residence time expressed by

$$\bar{t} = \int_0^{\infty} tE(t)dt \cong \sum_i^{\infty}\{t_i E_i \Delta t\} \qquad \text{.....(4-7)}$$

where E(t) is the residence time distribution function of the liquid in each stage given by [17]

$$E(t) = \frac{\beta}{\Gamma_2} e^{-\left(\frac{t}{\Gamma_2}\right)} + \frac{(1-\beta)}{\Gamma_1} e^{-\left(\frac{t}{\Gamma_1}\right)} \qquad \text{.....(4-8)}$$

where

$$\Gamma_1 = \frac{\Delta Z h_d}{(1-\beta)v_L} \qquad \text{.....(4-9)}$$

$$\Gamma_2 = \frac{\Delta Z h_s}{\beta v_L} \qquad \text{.....(4-10)}$$

ΔZ = height of a stage, [m]

β = fraction of the total liquid passing through the stagnant region, dimensionless

h_d = dynamic liquid hold-up in the column, $[m^3 \cdot m^{-3}]$

h_s = static liquid hold-up in the column, $[m^3 . m^{-3}]$

v_L = liquid velocity, (Equations 4-9 and 4-10) $[m . s^{-1}]$

t = residence time, [s]

The expression, E(t), suggested by Van Swaaij et al.[17] is a two-parameter model (β and n) in which these authors consider the column to be made up of a series of stages of height ΔZ so that in each stage, two parallel mixed cells are formed with mean residence time τ_1 and τ_2 , fed by a fraction ($1 - \beta$) and β of the total liquid flow rate respectively.

It is not possible to measure t_i directly by experiment or to calculate t_i from Equation 4-5. However, by assuming a very high number of streams, the stream residence time, t_i , will approach a mean residence time, $\bar{t}$, which is

$$t_i \longrightarrow \bar{t} = \frac{S\Delta Z \sum_i^{\infty} \{\delta h_i\}}{\sum_i^{\infty} q_i} \qquad \text{(4-11)}$$

$$i \longrightarrow \infty$$

Recognizing that

$$\sum_i^{\infty} \delta h_i = h_t \qquad \text{(4-12)}$$

and

$$\sum_i^{\infty} \delta q_i = Q \qquad \text{(4-13)}$$

represent the total liquid hold-up and total liquid flowrate respectively, we have

$$\bar{t} = \frac{S\Delta Zh_t}{Q} = \frac{\Delta Zh_t}{\frac{Q}{S}} \qquad \text{-----(4-14)}$$

or

$$\bar{t} = \frac{\Delta Zh_{t_2}}{v_L} \qquad \text{-----(4-15)}$$

Both ΔZ and v_L are measurable quantities and h_t can be determined from

$$h_t = h_d + h_s \qquad \text{-----(4-16)}$$

where h_d is the dynamic hold-up or operating hold-up corresponding to the liquid which flows rapidly over the packing surface. It is defined by the Otake and Okadas [17] correlation according to

$$h_d = \frac{1.295}{\epsilon}\left(\frac{dL}{\mu_L}\right)^{0.676} * \left(\frac{d^3 g \rho_L^2}{\mu_L^2}\right)^{-0.44} * S_p(1-\epsilon)d \qquad \text{-----(4-17)}$$

where h_d = dynamic hold-up in the column, $[m^3.m^{-3}]$

ϵ = porosity, (void fraction), dimensionless

d = nominal packing diameter, [m]

L = superficial liquid mass velocity, $[Kg.m^{-2}.s^{-1}]$

μ_L = liquid viscosity, $[Kg.m^{-1}.s^{-1}]$

ρ_L = liquid density, $[Kg.m^{-3}]$

g = acceleration due to gravity, $[m.s^{-2}]$

S_p = specific surface of a particle, $[m^2.m^{-3}]$

The static hold-up, h_s, corresponding to the stagnant liquid pockets in the column can be evaluated from the graphical correlation in Figure 4.1.

Having considered the stream residence time, let us first assume that each stream has an interfacial area $\{S\Delta Z\,\delta a_i\}$ in each stage, and then define the interfacial area per unit liquid volume for the i th stream as [4]

$$a_{Li} = \frac{S\Delta Z\,\delta a_i}{S\Delta Z\,\delta h_i} \qquad \text{-----(4-18)}$$

where δa_i = stream interfacial area per unit column volume, $[m^2 \cdot m^{-3}]$

From Equation 4-5, we have

$$S\Delta Z\delta h_i = t_i \delta q_i \qquad \text{-----(4-19)}$$

Consequently Equation 4-18 can be rewritten as [4]

$$a_{Li} = \frac{S\Delta Z\,\delta a_i}{t_i \delta q_i} \qquad \text{-----(4-20)}$$

The actual stream interfacial area a_{Li} between two phases is not known. However, for a very large number of streams, the stream interfacial area, a_{Li} will approach a mean value $\bar{a}_L$, given by

$$a_{Li} \underset{i \to \infty}{\longrightarrow} \bar{a}_L = \frac{S\Delta Z \sum_i^{\infty} \delta a_i}{S\Delta Z \sum_i^{\infty} \delta h_i} \qquad \text{-----(4-21)}$$

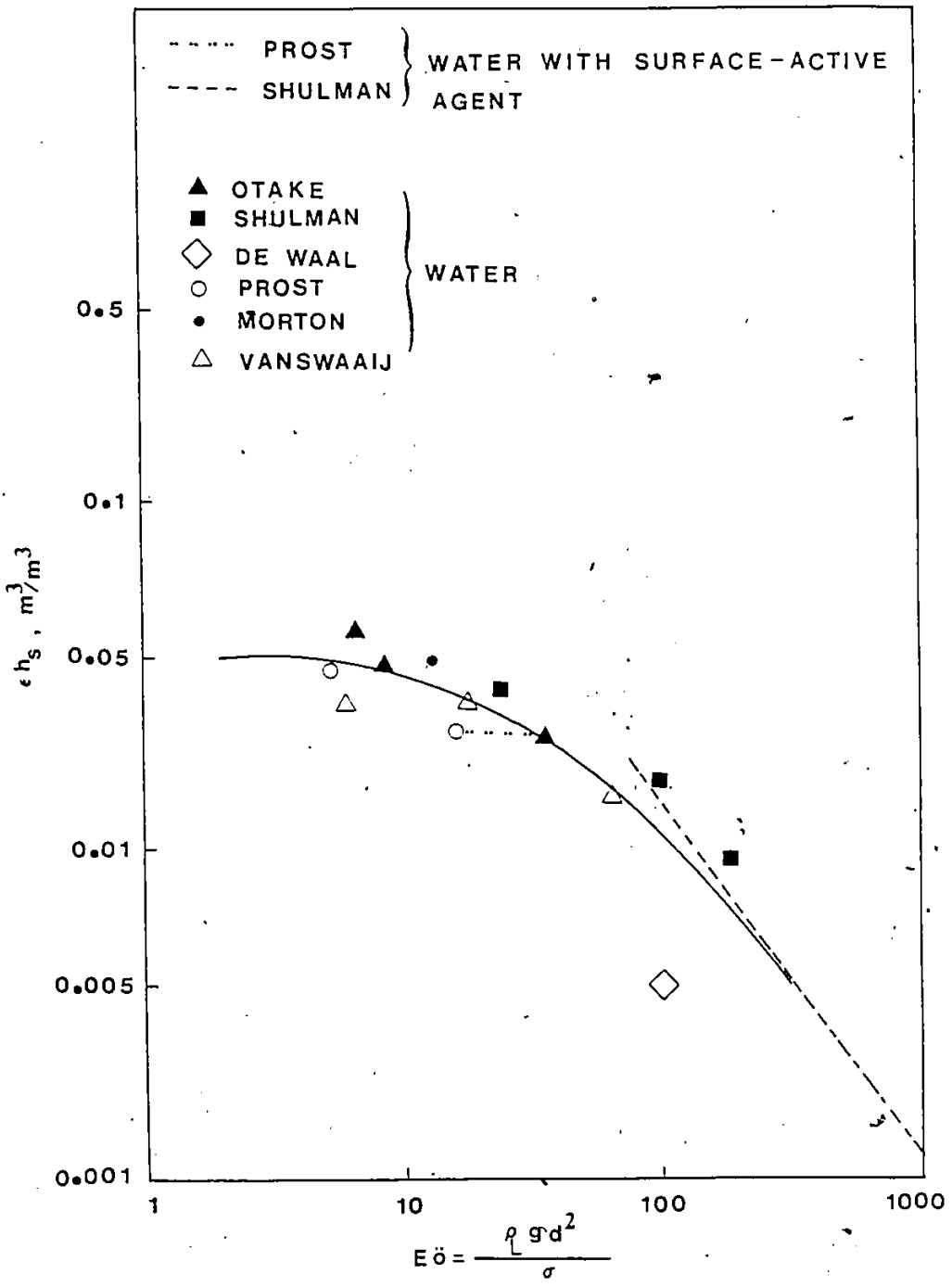

Figure 4-1 : Static Hold-Up Graphical Correlation (16) with the Eötvos Number

Recognizing that

$$\sum_i^{\infty} \delta a_i = a \qquad \text{-----(4-22)}$$

and

$$\sum_i^{\infty} \delta h_i = h_t \qquad \text{-----(4-23)}$$

are the total interfacial area per unit column volume and total liquid hold-up respectively, it follows that

$$\bar{a}_L = \frac{a}{h_t} \qquad \text{-----(4-24)}$$

By taking the wetted surface of the packing to be identical to the gas-liquid interface, it is possible to write

$$a = a_w \qquad \text{-----(4-25)}$$

and obtain

$$\bar{a}_L = \frac{a_w}{h_t} \qquad \text{-----(4-26)}$$

where the magnitude of a_w is given by Onda et al.[12] to be

$$\frac{a_w}{a_t} = 1 - \exp\left\{-1.45\left(\frac{\sigma_c}{\sigma}\right)^{0.75} * \left(\frac{L}{a_t \mu_L}\right)^{0.1} * \left(\frac{L^2 a_t}{\rho_L^2 g}\right)^{-0.05} * \left(\frac{L^2}{\rho_L \sigma a_t}\right)^{0.2}\right\}$$

-----(4-27)

where a_w = wetted surface area of packing per unit column volume, $[m^2 . m^{-3}]$

a_t = total surface area of packing per unit column volume, $[m^2 . m^{-3}]$

σ_c = critical surface tension of packing material, $[N.m^{-1}]$

σ = surface tension of liquid, $[N.m^{-1}]$

L = superficial liquid mass velocity, $[Kg.m^{-2}.s^{-1}]$

μ_L = liquid viscosity, $[Kg.m^{-1}.s^{-1}]$

ρ_L = liquid density, $[Kg.m^{-3}]$

g = acceleration due to gravity, $[m.s^{-2}]$

After considering the stream residence time and the stream interfacial area, we now assume in each stage j, a uniform molar fraction, $\bar{Y}_{A,j}$, of A in the gas phase to be given by [5]

$$\bar{Y}_{A,j} = \frac{1}{2}(Y_{A,j} + Y_{A,j+1}) \qquad \text{.....(4-28)}$$

where $\bar{Y}_{A,j}$ is a mean value between the molar fractions in the inlet ($Y_{A,j+1}$) and that in the outlet ($Y_{A,j}$) gas flow as shown in Figure 4-2.

Since the absorption of species A in the column will depend on its solubility and reaction in the liquid, the controlling resistance to mass transfer may occur in the liquid phase, in the gas phase or in both phases. These will be considered separately in the following sections.

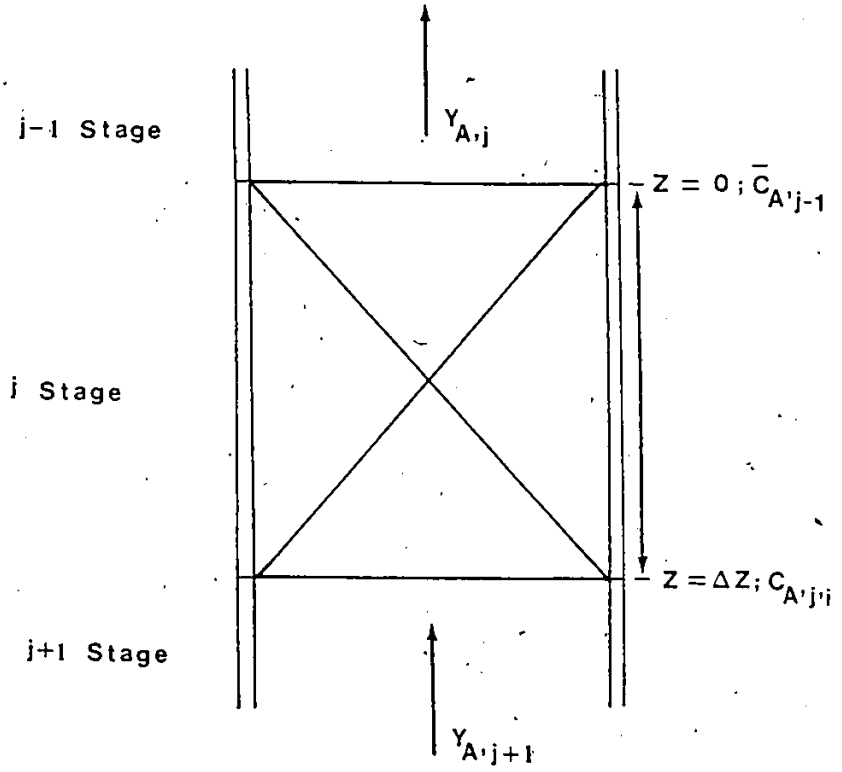

Figure 4-2 : A Schematic Diagram of A Stage

4.2.1 Physical Absorption Model

In the NO_X/SO_X - water system, where the dissolved gas species A does not react or reacts very slowly with water, the process described by Equation 4-3

$$\mathcal{F}_A A_L + \mathcal{F}_B B_L \longrightarrow \text{Product} \qquad \text{.....(4-3)}$$

is insignificant. For this case, we have physical absorption in the packed column. Furthermore if $k_G a >> k_L a$, we have physical absorption with controlling resistance dominated by the liquid phase so that gas phase resistance to absorption is negligible. According to Chang and Rochelle [18], and Komiyama and Inoue [19], this assumption is valid provided that $(k_L a)$ for the liquid phase is about 40 times smaller than $(k_G a)$ for the gas phase.

Using the general Equation 3-5 for mass transfer in a steady state operation, the local physical absorption rate of a component A in each liquid stream i, in any stage j is expressed by

$$k_G P_t \, (\bar{Y}_{A,j} - Y_A^*) = k'_{Li} \, (C_A^* - C_A) \qquad \text{.....(4-29)}$$

where k_G = gas phase mass transfer coefficient, assumed constant along the column, [Kmole.m^{-2}.s^{-1}.atm^{-1}]

P_t = total pressure of the system, [atm]

$\bar{Y}_{A,j}$ = mean molar fraction of component A defined by Equation 4-28, dimensionless

Y_A^* = molar fraction of component A at interface in equilibrium with C_A^*, dimensionless

k'_{Li} = local liquid phase mass transfer coefficient of stream i, considered constant along the stream path in the stage and is defined by

$$k'_{Li} = \frac{\mathcal{E}}{\sqrt{t_i}} \qquad \text{.....(4-30)}$$

where $\mathcal{E} = \sqrt{\frac{D_{LA}}{\pi}}$ is assumed constant for all streams.

The rate of change of mass of component A in each liquid stream i, in the same stage is given by

$$\delta q_i \Delta C_A \qquad \text{.....(4-31)}$$

Dividing Equation 4-31 by the stream interfacial area, $\{S\delta a_i \Delta Z\}$, in the stage and taking the limit as $\Delta Z \longrightarrow 0$, we have

$$N_A = \lim_{\Delta Z \longrightarrow 0} \frac{\delta q_i \Delta C_A}{S\delta a_i \Delta Z} = \frac{\delta q_i dC_A}{S\delta a_i dZ} \qquad \text{.....(4-32)}$$

From Equation 4-20, we get

$$\frac{\delta q_i}{\delta a_i} = \frac{S\Delta Z}{a_{Li} t_i} \qquad \text{.....(4-33)}$$

Substitution of Equation 4-33 into Equation 4-32, gives

$$N_A = \frac{\Delta Z dC_A}{a_{Li} t_i dZ} \qquad \text{.....(4-34)}$$

It is required from the mass balance on component A that Equation 4-29 and Equation 4-34 represent the same rate of absorption [5]. Therefore it is possible to write

$$k_G P_t (\bar{Y}_{A,j} - Y_A^*) = k'_{Li}(C_A^* - C_A) = \frac{\delta q_i dC_A}{S\delta a_i dZ} = \frac{\Delta Z dC_A}{a_{Li} t_i dZ} \qquad \text{.....(4-35)}$$

At the interface, if the operating pressure is not too high or too low, Henry's law is valid for a dilute system and the gas-liquid equilibrium can be expressed by

$$C_A^* = \frac{P_t Y_A^*}{H} \qquad \text{.....(4-36)}$$

where C_A^* = interfacial concentration of component A in liquid absorbent, [Kmole.m^{-3}]

P_t = total pressure of the system, [atm]

Y_A^* = molar fraction of component A at interface in equilibrium with C_A^*, dimensionless

H = Henry's law constant for component A, [atm.m^3.$Kmole^{-1}$]

Substitution of Equations 4-30, and 4-36 into 4-35, with rearrangement leads to a solution for C_A^*, in the form

$$C_A^* = \frac{1}{\mathcal{E} + Hk_G\sqrt{t_i}} \left\{ k_G \sqrt{t_i} P_t \bar{Y}_{A,j} + \mathcal{E} C_A \right\} \quad \text{--- (4-37)}$$

where $\mathcal{E} = \sqrt{\frac{D_{LA}}{\pi}}$. Further simplification provides

$$C_A^* = \frac{\sqrt{t_i}}{\mathcal{E} + Hk_G\sqrt{t_i}} \left\{ k_G P_t \bar{Y}_{A,j} + k'_{Li} C_A \right\} \quad \text{--- (4-38)}$$

By multiplying the numerator and denominator of Equation 4-38 by $(\sum_i^\infty \frac{q_i}{Q}\sqrt{t_i})$ and assuming a very high number of streams, C_A^* can be expressed by

$$C_A^* = \frac{\int_0^\infty t\, E(t)dt}{\mathcal{E}\int_0^\infty \sqrt{t}\, E(t)dt + Hk_G \int_0^\infty t\, E(t)dt} \left\{ k_G P_t \bar{Y}_{A,j} + k'_{Li} C_A \right\} \quad \text{------ (4-39)}$$

Since $\int_0^\infty t\, E(t)dt = \bar{t}$ according to Equation 4-7, this means that

$$C_A^* = \frac{\bar{t} \left\{ k_G P_t \bar{Y}_{A,j} + k'_{Li} C_A \right\}}{\mathcal{E}\int_0^\infty \sqrt{t}\, E(t)dt + Hk_G \bar{t}} \quad \text{------ (4-40)}$$

From Equation 4-8, it follows that

$$\int_0^\infty \sqrt{t}\, E(t)dt = \int_0^\infty \sqrt{t}\left\{\frac{\beta}{\Gamma_2} e^{-\frac{t}{\Gamma_2}} + \frac{(1-\beta)}{\Gamma_1} e^{-\frac{t}{\Gamma_1}}\right\}dt$$

which reduces to

$$\int_0^\infty \sqrt{t}\, E(t)dt = \frac{\beta}{2}\sqrt{\pi\Gamma_2} + \frac{(1-\beta)}{2}\sqrt{\pi\Gamma_1} \qquad \text{---(4-41)}$$

Substitution of Equation 4-41 into Equation 4-40, gives

$$C_A^* = \frac{\bar{t}\left\{k_G P_t \bar{Y}_{A,j} + k'_{Li} C_A\right\}}{\mathcal{E}\left\{\frac{\beta}{2}\sqrt{\pi\Gamma_2} + \frac{(1-\beta)}{2}\sqrt{\pi\Gamma_1}\right\} + Hk_G\bar{t}} \qquad \text{---(4-42)}$$

By multiplying the numerator and denominator of Equation 4-38 by $\left(\sum_i^\infty \frac{q_i}{Q}\right)$ and assuming a very high number of streams, we have

$$C_A^* = \frac{\int_0^\infty \sqrt{t}\, E(t)dt}{\mathcal{E}\int_0^\infty E(t)dt + Hk_G\int_0^\infty \sqrt{t}\, E(t)dt}\left\{k_G P_t \bar{Y}_{A,j} + k'_{Li} C_A\right\}$$

---(4-43)

Since

$$\int_0^\infty E(t)dt = 1$$

and

$$\int_0^\infty \sqrt{t}\, E(t)dt = \frac{\beta}{2}\sqrt{\pi\Gamma_2} + \frac{(1-\beta)}{2}\sqrt{\pi\Gamma_1}$$

according to Equations 4-6 and 4-41 respectively

Equation 4-43 can be rewritten in the form of

$$C_A^* = \frac{\left\{\frac{\beta}{2}\sqrt{\pi\Gamma_2} + \frac{(1-\beta)}{2}\sqrt{\pi\Gamma_1}\right\}\left\{k_G P_t \bar{y}_{A,j} + k_{Li} C_A\right\}}{\mathcal{E} + \left\{\frac{\beta}{2}\sqrt{\pi\Gamma_2} + \frac{(1-\beta)}{2}\sqrt{\pi\Gamma_1}\right\} H k_G} \quad \ldots.(4\text{-}44)$$

A comparision of Equations 4-42 and 4-44, yields

$$\frac{\bar{t}}{\left\{\frac{\beta}{2}\sqrt{\pi\Gamma_2} + \frac{(1-\beta)}{2}\sqrt{\pi\Gamma_1}\right\}} = \left\{\frac{\beta}{2}\sqrt{\pi\Gamma_2} + \frac{(1-\beta)}{2}\sqrt{\pi\Gamma_1}\right\} \quad \ldots.(4\text{-}45)$$

or

$$\bar{t} = \left\{\frac{\beta}{2}\sqrt{\pi\Gamma_2} + \frac{(1-\beta)}{2}\sqrt{\pi\Gamma_1}\right\}^2 \quad \ldots.(4\text{-}46)$$

Substitution of Equations 4-9, 4-10 and 4-15, into Equation 4-46, provides a determination of the liquid fraction, β, according to

$$\sqrt{\frac{4h_t}{\pi}} = \sqrt{h_s \beta} + \sqrt{(1-\beta)h_d} \quad \ldots.(4\text{-}47)$$

Assuming each stage is a perfect mixer so that the concentration of the dissolved component A in stream i will approach a mean value, $\bar{C}_{A,j-1}$, on leaving that stage, integration of Equation 4-35 for the j th-stage between, $\bar{C}_{A,j-1}$, the concentration of the component A in the liquid phase at Z=0

and $C_{A,j,i}$, the concentration at $Z = \Delta Z$ in the i th stream at the end of the stage, leads to

$$\mathcal{E} a_L \sqrt{t_i} \int_{Z=0}^{Z=\Delta Z} \frac{dZ}{\Delta Z} = \int_{\bar{C}_{A,j-1}}^{C_{A,j,i}} \frac{dC_A}{\left\{C_A^* - C_A\right\}} \quad \text{---(4-48)}$$

where $a_{Li} = a_L$, is the stream interfacial area per unit liquid volume and is assumed equal for all streams. Assuming ΔZ to be constant in the stage, Equation 4-48 becomes

$$\mathcal{E} a_L \sqrt{t_i} = \int_{\bar{C}_{A,j-1}}^{C_{A,j,i}} \frac{dC_A}{\left\{C_A^* - C_A\right\}} \quad \text{----(4-49)}$$

Substitution of Equation 4-38 into Equation 4-49, provides the relationship given by Sicardi and Baldi [5], for a gas phase controlled process in the form of

$$\frac{\mathcal{E} a_L t_i H k_G}{\mathcal{E} + H k_G \sqrt{t_i}} = \ell n \left\{ \frac{P_t \bar{Y}_{A,j} - H \bar{C}_{A,j-1}}{P_t \bar{Y}_{A,j} - H C_{A,j,i}} \right\} \quad \text{----(4-50)}$$

However, substitution of Equations 4-42 and 4-46 into Equation 4-49, leads to

$$\mathcal{E} a_L \sqrt{t_i} = \int_{\bar{C}_{A,j-1}}^{C_{A,j,i}} \frac{dC_A}{\left\{ \frac{\bar{t}(k_G P_t \bar{Y}_{A,j} + k_{Li} C_A)}{\mathcal{E}\sqrt{\bar{t}} + H k_G \bar{t}} \right\} - C_A} \quad \text{---(4-51)}$$

from which after letting

$$\mathcal{E}\sqrt{\bar{t}} + H k_G \bar{t} = \lambda \quad \text{----(4-52)}$$

it is possible to write

$$\frac{-\mathcal{E}a_L\sqrt{t_i}(k'_{Li}\bar{t}-\lambda)}{\lambda} = \ell n\left\{\frac{\bar{t}k_G P_t \bar{Y}_{A,j} + (k'_{Li}\bar{t}-\lambda)C_{A,j,i}}{\bar{t}k_G P_t \bar{Y}_{A,j} + (k'_{Li}\bar{t}-\lambda)\bar{C}_{A,j-1}}\right\} \quad \text{....(4-53)}$$

Solving for $C_{A,j,i}$ from Equation 4-53 and multiplying by $(\sum_i^{\infty}\frac{q_i}{Q})$ we obtain the mean concentration, $\bar{C}_{A,j}$, in the liquid leaving j th stage

$$\bar{C}_{A,j} = \frac{1}{\lambda - k'_{Li}\bar{t}}\left\{\bar{t}k_G P_t \bar{Y}_{A,j} - \left\{\bar{t}k_G P_t \bar{Y}_{A,j} - (\lambda - k'_{Li}\bar{t})\bar{C}_{A,j-1}\right\} * \exp\left\{\frac{\mathcal{E}a_L\sqrt{t_i}(\lambda - k'_{Li}\bar{t})}{\lambda}\right\}\right\} \quad \text{....(4-54)}$$

By assuming a very high number of streams, k'_{Li} will approach k_L, and t_i will approach $\bar{t}$ in the stage so that Equation 4-54 is reduced to

$$\bar{C}_{A,j} = \frac{1}{\lambda - k_L\bar{t}}\left\{\bar{t}k_G P_t \bar{Y}_{A,j} - \left\{\bar{t}k_G P_t \bar{Y}_{A,j} - (\lambda - k_L\bar{t})\bar{C}_{A,j-1}\right\} * \exp\left\{\frac{\mathcal{E}a_L\sqrt{\bar{t}}(\lambda - k_L\bar{t})}{\lambda}\right\}\right\} \quad \text{....(4-55)}$$

The quantities k_G and k_L are the gas side and liquid side mass transfer coefficients respectively which can be determined from the Onda, Sada and Takeuchi correlations [12]

$$\frac{k_G RT}{a_t D_{AG}} = 5.23 \left(\frac{G}{a_t \mu_G}\right)^{0.7} * \left(\frac{\mu_G}{\rho_G D_{AG}}\right)^{-\frac{1}{3}} * \left(\frac{a_t}{d_p}\right)^{-2} \quad \text{----(4-56)}$$

where k_G = gas side mass transfer coefficient, [Kmole.m^{-2}.s^{-1}.atm^{-1}]

R = gas constant, [atm.m^3 Kmole^{-1}.$^oK^{-1}$]

T = absolute temperature, [^oK]

a_t = total surface area of packing per unit column volume, [m^2.m^{-3}]

D_{AG} = gas phase molecular diffusivity of component A, [m^2.s^{-1}]

G = superficial mass velocity of gas, [Kg.m^{-2}.s^{-1}]

μ_G = gas viscosity, [Kg.m^{-1}.s^{-1}]

ρ_G = gas density, [Kg.m^{-3}]

d_p = diameter of a sphere having the same geometric surface area as the packing particle in question, [m], $d_p = \left(\frac{1 - \epsilon}{a_s}\right)$

$$k_L \left(\frac{\rho_L}{\mu_L g}\right)^{-\frac{1}{3}} = 0.0051 \left(\frac{L}{a_w \mu_L}\right)^{\frac{2}{3}} * \left(\frac{\mu_L}{\rho_L D_{AL}}\right)^{-\frac{1}{2}} * (a_t d_p)^{0.4} \quad \text{----(4-57)}$$

where k_L = liquid side mass transfer coefficient, [m.s^{-1}]

ρ_L = liquid density, [Kg.m^{-3}]

μ_L = liquid viscosity, [Kg.m^{-1}.s^{-1}]

g = acceleration due to gravity, [m.s^{-2}]

L = superficial liquid mass velocity, [Kg.m^{-2}.s^{-1}]

a_w = wetted surface area of packing per unit column volume, $[m^2 \cdot m^{-3}]$

D_{AL} = liquid phase molecular diffusivity of component A, $[m^2 \cdot s^{-1}]$

a_t = total surface area of packing per unit column volume, $[m^2 \cdot m^{-3}]$

d_p = diameter of a sphere having the same geometric surface area as the packing particle in question, [m]

The determination of $\bar{C}_{A,j}$ from Equation 4-55 facilitates the calculation of the physical absorption rate from [5]

$$(N_A a)_j = \frac{v_L}{\Delta Z} \left\{ \bar{C}_{A,j} - \bar{C}_{A,j-1} \right\} \qquad \text{----(4-58)}$$

where $(N_A a)_j$ is the physical absorption rate per unit column volume in stage j.

For the case of physical absorption with a liquid phase controlled process, we have $k_G >> k_L$ so that $\frac{k_L}{k_G} \cong 0$, and the expression for $\bar{C}_{A,j}$ given by Equation 4-55 reduces to

$$\bar{C}_{A,j} = \frac{1}{\left\{\frac{\lambda}{k_G}\right\}} \left| \bar{t} P_t \bar{Y}_{A,j} - \left(\bar{t} P_t \bar{Y}_{A,j} - \frac{\lambda}{k_G} \bar{C}_{A,j-1} \right) * \exp\left\{ \frac{\mathcal{E} a_L \sqrt{\bar{t}} (\lambda - k_L \bar{t})}{\lambda} \right\} \right| \qquad \text{----(4-59)}$$

Our model for physical absorption is completed at this point. However, if absorption of gaseous component A is coupled with an irreversible chemical reaction in the liquid phase, a different expression for $\bar{C}_{A,j}$ other than Equations 4-55 and 4-59, will be expected. This case is considered in the next section.

4.2.2 Chemical Absorption Model

In the NO_x/SO_x - mixed sodium hydroxide and sodium chlorite solution system, the dissolved gaseous component A reacts irreversibly with species B so that the process described by Equation 4-3

$$\mathcal{F}_A A_L + \mathcal{F}_B B_L \longrightarrow \text{Product} \qquad \text{----(4-3)}$$

is significant. For the case of chemical absorption in a column, Chang and Rochelle [18], and Komiyama and Inoue [19], suggest the liquid phase resistance to absorption is negligible provided that ($k_L a$) exceeds ($k_G a$) by a factor of about 250.

Using the general expression, Equation 3-6, for mass transfer in a steady state operation, the local chemical absorption rate of component A in each liquid stream i in any stage j can be expressed by

$$k_G P_t(\bar{Y}_{A,j} - Y_A^*) = \emptyset k'_{Li}(C_A^* - C_A) \qquad \text{-----(4-60)}$$

From Equation 1 and the stoichiometric requirement of Equation 4-3, we ave

$$\delta\Delta C_A = \delta q_i - \frac{\mathcal{F}_A}{\mathcal{F}_B}\Delta C_B \qquad \text{.....(4-61)}$$

Equations 4-32, 34, 4-60, 4-61 and the mass balance on component A in ste j enable us to write

$$k_G P_t(\bar{Y}_{A,j} - Y_A^*) = \phi k'_{Li}(C_A^* - C_A) = -\left\{\frac{\int_0^{\Delta Z} \mathcal{F}_A dC_B}{a_{Li} t_i \mathcal{F}_B dZ}\right\} \qquad \text{.....(4-62)}$$

If we assu that the reaction is sufficiently fast, the concentration, $_A$, in the bulk liquid becomes zero. As a result, Equation -62 is reduced to

$$k_G P_t(\bar{Y}_{A,j} - Y_A^*) = \phi k'_{Li} C_A^* = -\left\{\frac{\Delta Z}{a_{Li} t_i}\right\}\frac{\mathcal{F}_A dC_B}{\mathcal{F}_B dZ} \qquad \text{.....(4-63)}$$

Depending on the absorption conditions, different models may arise at this point. The sections that follow will discuss the chemical absorption models concerned with

1. removal of NO alone.
2. removal of SO_2 alone.
3. simultaneous removal of NO and SO_2 with aqueous mixed sodium hydroxide and sodium chlorite solution.

4.2.2.1 NO - ($NaClO_2$ + NaOH) System

According to Sada et al. [20,21], the reaction between nitric oxide and chlorite ion in an alkaline solution is considered to be

$$2NO + ClO_2^- \lessgtr\!=\!=\!=\!=\!=\!=\!\gtrless 2NO_2 + Cl^- \qquad \text{.....(4-64)}$$

$$4NO_2 + ClO_2^- + 4OH^- \lessgtr\!=\!=\!=\!=\!=\!\gtrless 4NO_3^- + Cl^- + 2H_2O \qquad \text{.....(4-65)}$$

The overall reaction is

$$4NO + 3ClO_2^- + 4OH^- \lessgtr\!=\!=\!=\!=\!\gtrless 4NO_3^- + 3Cl^- + 2H_2O \qquad \text{.....(4-66)}$$

Sada et al.[20,21], who confirmed that the system operates under the fast reaction regime, expressed the local absorption rate by the film model in terms of

$$N_{A_2} = \sqrt{\frac{2}{3} k_3 C_{B_1} C_{A_2}^{*\,3} D_{A_2} L} \qquad \text{.....(4-67)}$$

where the subscripts A_2 and B_1 refer to nitric oxide (NO) and sodium chlorite ($NaClO_2$) respectively in this section and k_3 is the third order rate constant with a value of $2.1*10^{12}$ $(m^3.Kmole^{-1})^2.s^{-1}$ at 25 °C. The value of k_3 can also calculate from the empirical correlation [20,21]

$$k_3 = 3.8x10^{12} Exp\,(-3.73 C_{B_2}^{o}) \qquad \text{.....(4-68)}$$

for the range $0.05 < C_{B_2}^{o} < 0.5$ molar where $C_{B_2}^{o}$ is the initial sodium hydroxide concentration in the solution.

The criterion for the fast-reaction regime as given by Danckwerts [22], takes the form

$$\frac{\sqrt{k_3 \bar{C}_{B_1,j-1} C^*_{A_2} D_{A_2L}}}{k_L} >> 1 + \frac{\mathcal{F}_{A_2} \bar{C}_{B_1,j-1}}{\mathcal{F}_{B_1} C^*_{A_2}} \qquad \text{----(4-69)}$$

where the values of $C^*_{A_2}$ and D_{A_2L} can be estimated from the correlations given in Appendix A.

The mass balance requires that the rate of absorption of component A in any stage j, expressed by Equations 4-63 and 4-67, must be equal. Therefore, it is possible to write

$$\sqrt{\frac{2}{3} k_3 C_{B_1} C^{*3}_{A_2} D_{A_2L}} = \emptyset k'_{Li} C^*_{A_2} = - \frac{\Delta Z}{a_{Li} t_i} \frac{\mathcal{F}_{A_2} dC_{B_1}}{\mathcal{F}_{B_1} dZ} \qquad \text{----(4-70)}$$

where the enhancement factor, $\emptyset$, in this case is defined by

$$\emptyset = \frac{\sqrt{\frac{2}{3} k_3 C_{B_1} C^*_{A_2} D_{A_2L}}}{k'_{Li}} \qquad \text{----(4-71)}$$

Integration of Equation 4-70 for the j th stage between $\bar{C}_{B_1,j-1}$, the concentration of the absorbent ($NaClO_2$) in the liquid phase at Z=0 and $C_{B_1,j,i}$, the concentration at $Z = \Delta Z$ in the i th stream at the end of the stage, leads to

$$\frac{a_{Li} t_i \mathcal{F}_{B_1} \sqrt{\frac{2}{3} k_3 C^{*3}_{A_2} D_{A_2L}}}{\mathcal{F}_{A_2}} \int_{Z=0}^{Z=\Delta Z} \frac{dZ}{\Delta Z} = - \int_{\bar{C}_{B_1,j-1}}^{C_{B_1,j,i}} \frac{dC_{B_1}}{\sqrt{C_{B_1}}}$$

$$\qquad \text{----(4-72)}$$

Assuming ΔZ to be constant throughout the stage, Equation 4-72 becomes

$$C_{B_1,j,i} = \left\{ \sqrt{\bar{C}_{B_1,j-1}} - \frac{a_{Li} t_i \mathcal{F}_{B_1} \sqrt{\frac{2}{3} k_3 C_{A_2}^{*3} D_{A_2 L}}}{2\mathcal{F}_{A_2}} \right\}^2 \qquad \text{------(4-73)}$$

The assumption of a very high number of streams yields

$$\text{i.} \quad \sum_i^{\infty} \frac{q_i}{Q} = \int_0^{\infty} E(t)dt = 1$$

$$\text{ii.} \quad \sum_i^{\infty} \frac{q_i}{Q} t_i = \int_0^{\infty} tE(t)dt = \bar{t}$$

$$\text{iii.} \quad \underset{i \to \infty}{a_{Li}} \longrightarrow \bar{a}_L$$

so that by multiplication of Equation 4-73 by $\left(\sum_i^{\infty} \frac{q_i}{Q} \right)$, we obtain the expression for, $\bar{C}_{B_1,j}$, the mean concentration in the liquid stream leaving the j th stage to be

$$\bar{C}_{B_1,j} = \left\{ \sqrt{\bar{C}_{B_1,j-1}} - \frac{\bar{a}_L \bar{t} \mathcal{F}_{B_1} \sqrt{\frac{2}{3} k_3 C_{A_2}^{*3} D_{A_2 L}}}{2\mathcal{F}_{A_2}} \right\}^2 \qquad \text{------(4-74)}$$

The rate of chemical absorption for the $NO-(NaClO_2 + NaOH)$ system per unit column volume in stage j, is calculated from

$$(N_{A_2} a)_j = \frac{V_L}{\int \Delta Z} \left\{ \bar{C}_{B_1,j-1} - \bar{C}_{B_1,j} \right\} \qquad \text{------(4-75)}$$

where $\bar{C}_{B_1,j-1}$ and $\bar{C}_{B_1,j}$ are determined from Equation 4-74.

4.2.2.2 SO_2 - ($NaClO_2$ + NaOH) System

When sulfur dioxide is absorbed into aqueous alkaline chlorite solution, the following reactions occur :

$$SO_{2(g)} \leqslant\!\!=\!\!=\!\!=\!\!=\!\!=\!\!=\!\!=\!\!\geqslant SO_{2(soln)} \qquad \text{-----(4-76)}$$

$$SO_{2(soln)} + OH^- \leqslant\!\!=\!\!=\!\!=\!\!=\!\!=\!\!=\!\!=\!\!\geqslant HSO_3^- \qquad \text{-----(4-77)}$$

$$HSO_3^- + OH^- \leqslant\!\!=\!\!=\!\!=\!\!=\!\!=\!\!=\!\!=\!\!\geqslant SO_3^{-2} + H_2O \qquad \text{-----(4-78)}$$

$$2SO_3^{-2} + ClO_2^- \leqslant\!\!=\!\!=\!\!=\!\!=\!\!=\!\!=\!\!\geqslant 2SO_4^{-2} + Cl^- \qquad \text{-----(4-79)}$$

According to Sada et al.[21], for sodium chlorite concentrations below 0.15 molar and partial pressures of SO_2 in the system varying between 0.0012 and 0.011 atmosphere, the rate of absorption was found to be completely under gas-film control. The local rate of reaction is believed to be first order with respect to the SO_2 and OH^- concentrations. Therefore, the overall order is of the second power with the rate constant, k_2, being equal to $3.64*10^8$ $l.mole^{-1}.s^{-1}$ ($m^3.Kmole^{-1}.s^{-1}$) [23]. Since this process was confirmed to occur in the fast reaction regime, it can be argued that gas film controlling resistance prevails [24]. According to Danckwerts [21], the local rate of SO_2 absorption in any stream i, can be expressed by the film model

$$N_{A_1} = \sqrt{k_2 C_{B_2} C_{A_1}^{*2} D_{A_1} L} \qquad \text{------(4-80)}$$

where subscripts A_1 and B_2 refer to SO_2 and NaOH respectively in this section. The validity of the fast reaction regime can be checked further by Equation 4-81 which shows that [22]

$$\frac{\sqrt{k_2 \bar{C}_{B_2,j-1} C^*_{A_1} D_{A_1L}}}{k_L} \gg 1 + \frac{\mathcal{F}_{A_1} \bar{C}_{B_2,j-1}}{\mathcal{F}_{B_2} C^*_{A_1}} \qquad \text{---(4-81)}$$

Values of $C^*_{A_1}$ and D_{A_1L} can be estimated by the method given in Appendix A.

According to the mass balance on component A in any stage j, the rates of absorption as given by Equations 4-63 and 4-80 must be equal for the system under discussion. Consequently

$$\sqrt{k_2 C_{B_2} C^{*2}_{A_1} D_{A_1L}} = \emptyset k'_{Li} C^*_{A_1} = -\frac{\Delta Z}{a_{Li} t_i} \frac{\mathcal{F}_{A_1} dC_{B_2}}{\mathcal{F}_{B_2} dZ} \qquad \text{---(4-82)}$$

where the enhancement factor, $\emptyset$, in the present case is defined by

$$\emptyset = \frac{\sqrt{k_2 C_{B_2} D_{A_1L}}}{k'_{Li}} \qquad \text{------(4-83)}$$

Integration of Equation 4-82 for the j th stage between $\bar{C}_{B_2,j-1}$, the concentration of the absorbent B_2 (NaOH) in the liquid phase at Z = 0 and, $C_{B_2,j,i}$, the concentration at

$Z = \Delta Z$ in the i th stream at the end of the stage, leads to

$$\frac{a_{Li} t_i \mathcal{F}_{B_2} \sqrt{k_2 C_{A_1}^{*2} D_{A_1 L}}}{\mathcal{F}_{A_1}} \int_{Z=0}^{Z=\Delta Z} \frac{dZ}{\Delta Z} = \int_{\bar{C}_{B_2,j-1}}^{C_{B_2,j,i}} - \frac{dC_{B_2}}{\sqrt{C_{B_2}}} \quad \ldots (4\text{-}84)$$

Assuming ΔZ to be constant throughout the stage, Equation 4-84 becomes

$$C_{B_2,j,i} = \left\{ \sqrt{\bar{C}_{B_2,j-1}} - \frac{a_{Li} t_i \mathcal{F}_{B_2} \sqrt{k_2 C_{A_1}^{*2} D_{A_1 L}}}{2 \mathcal{F}_{A_1}} \right\}^2 \quad \ldots (4\text{-}85)$$

Multiplication of Equation 4-85 by $(\sum_i^{\infty} \frac{q_i}{Q})^2$ and the assumption of a very high number of streams yields, $\bar{C}_{B_2,j}$, the mean concentration in the liquid stream leaving the j th stage, in the form of

$$\bar{C}_{B_2,j} = \left\{ \sqrt{\bar{C}_{B_2,j-1}} - \frac{\bar{a}_L \bar{t} \mathcal{F}_{B_2} C_{A_1}^{*} \sqrt{k_2 D_{A_1 L}}}{2 \mathcal{F}_{A_1}} \right\}^2 \quad \ldots (4\text{-}86)$$

Consequently the rate of chemical absorption for the SO_2-($NaClO_2$ +NaOH) system per unit column volume in the stage j is given by Equation 4-87, with $\bar{C}_{B_2,j-1}$ and $\bar{C}_{B_2,j}$ determined from Equation 4-86.

$$(N_{A_1} a)_j = \frac{v_L}{\Delta Z} \left\{ \bar{C}_{B_2,j-1} - \bar{C}_{B_2,j} \right\} \quad \ldots (4\text{-}87)$$

4.2.2.3 ($NO + SO_2$) - ($NaClO_2 + NaOH$) System

When both SO_2 (A_1) and NO (A_2) are absorbed simultaneously in aqueous mixed solutions of $NaClO_2$ (B_1) and NaOH (B_2), the presence of SO_2 will reduce the rate of NO absorption. At the gas-liquid interface, SO_2 will compete with NO for OH^- and ClO_2^- ions through reactions 4-88 and 4-89.

$$SO_2 + 2OH^- \lessgtr\!=\!=\!=\!=\!=\!\gtrless SO_3^{-2} + H_2O \qquad \text{.....(4-88)}$$

$$2SO_3^{-2} + ClO_2^- \lessgtr\!=\!=\!=\!=\!=\!=\!\gtrless 2SO_4^{-2} + Cl^- \qquad \text{.....(4-89)}$$

while NO removal occurs by way of

$$2NO + ClO_2^- \lessgtr\!=\!=\!=\!=\!=\!=\!\gtrless 2NO_2 + Cl^- \qquad \text{.....(4-90)}$$

$$4NO_2 + ClO_2^- + 4OH^- \lessgtr\!=\!=\!=\!=\!=\!\gtrless 4NO_3^- + Cl^- + 2H_2O \qquad \text{.....(4-91)}$$

The reduction of the NO absorption rate in the presence of SO_2 was confirmed by Sada et al.[21]. According to the Sada et al.[21] findings, it is likely that the simultaneous absorption of these two gases is under depletion conditions.

According to Ramachandran et al. [3], the criteria for defining depletion conditiors are expressed by

$$\frac{\sqrt{M_{A_1}}}{q_{A_1}} + \frac{\sqrt{M_{A_2}}}{q_{A_2}} \leq 1 + \frac{1}{q_{A_1A_2}} \qquad \text{.....(4-92)}$$

where

$$M_{A_1} = \frac{\left\{k_2 \bar{C}_{B_2,j-1} D_{A_1L}\right\}}{k_L^2} \qquad \text{.....(4-93)}$$

$$M_{A_2} = \frac{\left\{\frac{2}{3} k_3 \bar{C}_{B_1,j-1} C^*_{A_2} D_{A_2L}\right\}}{k_L^2} \quad \text{....(4-94)}$$

$$q_{A_1} = \frac{\bar{C}_{B_2,j-1}}{2C^*_{A_1}} \frac{D_{B_2L}}{D_{A_1L}} \quad \text{....(4-95)}$$

$$q_{A_2} = \frac{\bar{C}_{B_2,j-1}}{C^*_{A_2}} \frac{D_{B_2L}}{D_{A_2L}} \quad \text{....(4-96)}$$

$$q_{A_1A_2} = \bar{C}_{B_2,j-1} \left\{ 2C^*_{A_1} \frac{D_{A_1L}}{D_{B_2L}} + C^*_{A_2} \frac{D_{A_2L}}{D_{B_2L}} \right\}^{-1} \quad \text{....(4-97)}$$

where k_2 = second order rate constant, [$3.64*10^8$ $(l.mole^{-1}).s^{-1}$] with respct to the overall reaction of Eqs 4-76 to 4-79.

k_3 = third order rate constant, [$2.1*10^{12}$ $(m^3.Kmole^{-1})^2.s^{-1}$] with respect to Eq. (4-66)

The interfacial concentrations ($C^*_{A_1}$ and $C^*_{A_2}$) and the liquid phase diffusivities (D_{A_1L} and D_{A_2L}) of the absorbing gases can be estimated by the method given in Appendix A. The liquid-phase diffusivities of the reactants, ClO_2^- (D_{B_1L}) and OH^- (D_{B_2L}) are available in the literature [21], ($D_{B_1L} = 1.72*10^{-5}$ $cm^2.s^{-1}$; $D_{B_2L} = 3.34*10^{-5} cm^2.s^{-1}$). The unknown quantities are $\bar{C}_{B_1,j-1}$ and $\bar{C}_{B_2,j-1}$. However, their values can be calculated from the discussion that follows.

According to Sada et al.[21], the local rate of absorption of SO_2 into aqueous mixed solutions of sodium chlorite and sodium hydroxide in the presence of NO in stream i, can be expressed by

$$N_{A_1} = 2k_{L,ClO_2^-}\left\{\bar{C}_{B_1,j-i} - \bar{C}^*_{B_1}\right\} = \frac{1}{2}\,k_{L,OH^-}\left\{\bar{C}_{B_{2,j-1}} - \bar{C}^*_{B_2}\right\} \quad \ldots\ldots (4\text{-}98)$$

where the coefficients 2 and 1/2 on the right-hand sides of Equation 4-98 are derived from reciprocals of stoichiometric factors based on the reactions depicted by Equations 4-99 and 4-100. The values of k_{L,ClO_2^-} and k_{L,OH^-} are available in the literature [21], ($k_{L,ClO_2^-} = 2.18*10^{-3}$ cm.s^{-1} ; $k_{L,OH^-} = 4.23*10^{-3}$ cm.s^{-1}).

$$SO_2 + 2OH^- \lessequalgtr SO_3^{-2} + H_2O \qquad \ldots\ldots (4\text{-}99)$$

$$2SO_3^{-2} + ClO_2^- \lessequalgtr 2SO_4^{-2} + Cl^- \qquad \ldots\ldots (4\text{-}100)$$

For the simultaneous absorption of two gases under depletion conditions, the interfacial concentration, $C^*_{B_i}$, of the reactant B_i (i = 1,2), is given by [3]

$$C^*_{B_i} = C^o_{B_i} + \left\{2C^*_{A_1}\frac{D_{A_1L}}{D_{B_iL}}\right\} + \left\{C^*_{A_2}\frac{D_{A_2L}}{D_{B_iL}}\right\} - \left\{\frac{2N_{A_1}}{\{k_{1,A_1}\}_{Phy}} * \frac{D_{A_1L}}{D_{B_iL}}\right\} - \left\{\frac{N_{A_2}}{\{k_{L,A_2}\}_{Phy}} * \frac{D_{A_2L}}{D_{B_iL}}\right\} \quad \ldots\ldots (4\text{-}101)$$

where N_{A_1} and N_{A_2} are given by Equations 4-80 and 4-67 respectively.

Since the mass balance requires that the rate of absorption of component A in any stage j must be the same whether given by Equations 4-63 or 4-98, it is possible to write

$$\frac{1}{2} k_{L,OH^-} \left\{ \bar{C}_{B_2,j-1} - C^*_{B_2} \right\} = - \frac{\Delta Z}{a_{Li} t_i} \frac{\mathfrak{F}_{A_1}}{\mathfrak{F}_{B_2}} \frac{dC_{B_2}}{dZ} \qquad \text{---(4-102)}$$

Substitution of Equations 4-67, 4-80, and 4-101 (for i = 2) into Equation 4-102 and letting

$$\Phi_1 = \frac{1}{2} k_{L,OH^-} \left(\frac{a_{Li} t_i \mathfrak{F}_{B_2}}{\mathfrak{F}_{A_1}} \right) \qquad \text{----(4-103)}$$

$$\Phi_2 = C^o_{B_2} + 2C^*_{A_1} \frac{D_{A_1L}}{D_{B_2L}} + C^*_{A_2} \frac{D_{A_2L}}{D_{B_2L}} \qquad \text{----(4-104)}$$

$$\Phi_3 = \frac{2}{\{k_{L,A_1}\}_{Phy}} \frac{D_{A_1L}}{D_{B_2L}} \sqrt{k_2 C^{*2}_{A_1} D_{A_1L}} \qquad \text{----(4-105)}$$

$$\Phi_4 = \frac{1}{\{k_{L,A_2}\}_{Phy}} \frac{D_{A_2L}}{D_{B_2L}} \sqrt{\frac{2}{3} k_3 C^{*3}_{A_2} D_{A_2L}} \qquad \text{----(4-106)}$$

it is possible to re-write Equation 4-102 in the form of

$$\Phi_1 \left\{ \bar{C}_{B_2,j-1} - \Phi_2 + \Phi_3 \sqrt{C_{B_2}} + \Phi_4 \sqrt{C_{B_1}} \right\} = - \Delta Z \frac{dC_{B_2}}{dZ} \quad \text{.....(4-107)}$$

Assuming Φ_1, Φ_2, Φ_3 and Φ_4 are constant throughout a stage, integration of Equation 4-107 for the j th stage between $\bar{C}_{B_1,j-1}$, the concentration of the liquid reactant (NaOH) in the liquid phase at $Z = 0$, and $C_{B_2,j,i}$, the concentration at $Z = \Delta Z$ in the i th stream at the end of the stage, leads to

$$\Phi_1 \int_{Z=0}^{Z=\Delta Z} \frac{dZ}{\Delta Z} = - \int_{\bar{C}_{B_2,j-1}}^{C_{B_2,j,i}} \frac{dC_{B_2}}{\left\{ \bar{C}_{B_2,j-1} - \Phi_2 + \Phi_3 \sqrt{C_{B_2}} + 4 \sqrt{C_{B_1}} \right\}} \quad \text{----(4-108)}$$

On the right-hand side of Equation 4-108, there are two variables, namely C_{B_2} and C_{B_1}, which are changing throughout the stage. Treating C_{B_1} as a constant and integrating Equation 4-108 with respect to C_{B_2} while assuming that ΔZ is constant throughout the stage, leads to

$$\Phi_1 = - 2 \left\{ \frac{\sqrt{C_{B_2}}}{\Phi_3} - \frac{\Phi_4 \sqrt{C_{B_1}} + \bar{C}_{B_2,j-1} - \Phi_2}{\Phi_3^2} \left\{ \ell n \left\{ \Phi_4 \sqrt{C_{B_1}} + \bar{C}_{B_2,j-1} - \Phi_2 + \Phi_3 \sqrt{C_{B_2}} \right\} \right\} \right\| \begin{matrix} C_{B_2,j,i} \\ \bar{C}_{B_2,j-1} \end{matrix} + F(C_{B_1}) \quad \text{------(4-109)}$$

It can be shown from the Taylor expansion that

$$\ell n\{\Phi_4\sqrt{C_{B_1}} + \bar{C}_{B_{2,j-1}} - \Phi_2 + \Phi_3\sqrt{C_{B_2}}\} \cong \ell n\{\Phi_4\sqrt{C_{B_1}} + \bar{C}_{B_{2,j-1}}\} + \left\{\frac{\Phi_3\sqrt{C_{B_2}} - \Phi_2}{\Phi_4\sqrt{C_{B_1}} + \bar{C}_{B_{2,j-1}}}\right\} + \cdots \quad \text{---(4-110)}$$

provided that

$$\left|\frac{\Phi_3\sqrt{C_{B_2}} - \Phi_2}{\Phi_4\sqrt{C_{B_1}} + \bar{C}_{B_{2,j-1}}}\right| < 1 \quad \text{---(4-111)}$$

It is apparent that $F(C_{B_1})$ is a function given by Equation 4-73 in the form

$$F(C_{B_1}) = \left\{\sqrt{\bar{C}_{B_{1,j-1}}} - \frac{a_{Li}t_i\mathfrak{F}_{B_1}\sqrt{\frac{2}{3}k_3 C_{A_2}^{*3} D_{A_2L}}}{2\mathfrak{F}_{A_2}}\right\}^2 \quad \text{---(4-112)}$$

Substitution of Equation 4-110 into Equation 4-109, with subsequent solution for $\sqrt{C_{B_{2,j,i}}}$, yields

$$\sqrt{C_{B_{2,j,i}}} = \sqrt{\bar{C}_{B_{2,j-1}}} + \frac{\Phi_3}{2\Phi_2}\left\{\Phi_4\sqrt{C_{B_1}} + \bar{C}_{B_{2,j-1}}\right\} * \left\{F(C_{B_1}) - \Phi_1\right\} \quad \text{---(4-113)}$$

Subsititution of Equation 4-112 into Equation 4-113 with recognition that C_{B_1} is the same as $C_{B_{1,j,i}}$, facilitates multiplication of Equation 4 - 113 by $\left(\sum_{i}^{\infty} \frac{q_i}{Q} \right)$ to give

$$\sqrt{\bar{C}_{B_{2,j}}} \simeq \sqrt{\bar{C}_{B_{2,j-1}}} + \frac{\Phi_3}{2\,\Phi_2}\left\{\Phi_4 \sqrt{\bar{C}_{B_{1,j}}} + \bar{C}_{B_{2,j-1}}\right\} * \left\{\left\{\sqrt{\bar{C}_{B_{1,j-1}}} - \frac{\bar{a}_L \bar{t} \mathfrak{F}_{B_1} \sqrt{\frac{2}{3} k_3 C_{A_2}^{*3} D_{A_2 L}}}{2\,\mathfrak{F}_{A_2}}\right\}^2 - \hat{\Phi}_1\right\} \quad \text{.....(4-114)}$$

where

$$\hat{\Phi}_1 \simeq \frac{1}{2} k_{L,OH^-} \left\{\frac{\bar{a}_L \bar{t} \mathfrak{F}_{B_2}}{\mathfrak{F}_{A_1}}\right\} \quad \text{.....(4-115)}$$

The determination of $\bar{C}_{B_{2,j-1}}$ and $\bar{C}_{B_{2,j}}$ from Equation 4-114 enables us to calculate the rate of chemical absorption for the $(NO + SO_2)$ - $(NaClO_2 + NaOH)$ system from

$$(N_{A_1} a)_j = \frac{v_L}{\Delta Z}\left\{\bar{C}_{B_{2,j-1}} - \bar{C}_{B_{2,j}}\right\} \quad \text{.....(4-116)}$$

At this point, the models for chemical absorption are completed. The chapter that follows will describe the experimental program needed to validate these models.

REFERENCES

1. Brian P.L.T., Hurley J.F., and Hasseltine E.H., Penetration Theory for Gas-Absorption Accompanied by a Second Order Chemical Reaction. A.I.Ch. E. Journal, 7, pp.226 - 231, (June, 1961).

2. Roper G.H., Hatch T.F., and Pigford R.L., Theory of Absorption and Reaction of Two Gases in a Liquid. I. & E. C. Fundamentals, 1, pp.144-152, (May, 1962).

3. Ramachandran P.A., Sharma M.M., Simultaneous Absorption of Two Gases. Trans. Instn Chem. Engrs, 49, pp.253-260, (1971).

4. Baldi G., and Sicardi S., A Model for Mass Transfer With and Without Chemical Reaction in Packed Towers. Chemical Engineering Science, 30, pp.617-624, (1975).

5. Sicardi S., and Baldi G., A Model for Mass Transfer in Packed Towers : Mass Transfer with Controlling Resistance in the Gas Phase, Chemical Engineering Science, 31, pp.651-656, (1976).

6. Barreto G.F., An Approximate Solution to the Simulatneous Chemical Absorption of Two Gases. One Gas Reacts Instantaneously. The Chemical Engineering Journal, 24, pp. 81-87, (1982).

7. Van Krevelen D.W., and Hoftizer P.J., Kinetics of Simulta-neous Absorption and Chemical Reaction. Chemical Engineering Progress, 44, pp.529-536, (July, 1948).

8. Yoshida F., and Koyanagi T., Liquid Phase Mass transfer Rates and Effective Interfacial Area in Packed Absorption Columns. Industrial and Engineering Chemistry, 50, pp.365-374, (March, 1958).

9. Onda K., Sada E., and Murase Y., Liquid-Side Mass Transfer Coefficients in Packed Towers. A.I.Ch.E. Journal, 5, pp.235-239, (June, 1959).

10. Shulman H.L., Savini C.G., and Edwin R.V., Performance of Packed Columns VII. The Effect of Hold-Up on Gas-Phase Mass Transfer Rates. A.I.Ch. E. Journal, 9, pp.479-484, (July, 1963).

11. Onda K., Takeuki H., and Okumoto Y., Mass Transfer Coefficients Between Gas and Liquid-Phases in Packed Columns. Journal of Chemical Engineering of Japan, 1, pp.56-62, (1968).

12. Onda K., Sada E., and Takeuchi H., Gas Absorption with Chemical Reaction in Packed Columns. Journal of Chemical Engineering of Japan, 1, pp.62-66, (1968).

13. Shulman H.L., Mellish W.G., and Lyman W.H., Performance of Packed Columns : IX. Simulation of a Packed Column. A.I.Ch.E. Journal, 17, pp.631-640, (1971).

14. Michell R.W., and Furzer I.A., Trickle Flows in Packed Beds. Trans. Instn. Chem. Engrs, 50, pp.334-342, (1972).

15. De Wall K.I.A., and Van Mameren, A.C., Proceedings of The Symposium on Transport Phenomena. Institution of Chemical Engineers, London, pp.60, (1965).

16. Levenspiel O., Chemical Reaction Engineering. 2nd Ed., pp.255, 261, John Wiley & Son Inc., New York, (1972).

17. Van Swaaij W.P.M., Charpentier J.C., and Villermaux J., Residence Time Distribution in Liquid Phase of Trickle Flow in Packed Columns. Chemical Engineering Science, 24, pp.1083-1095, (1969).

18. Chang C.S., and Rochelle G.T., SO_2 Absorption into Aqueous Solutions. A.I.Ch. E. Journal, 27, pp.292-298, (March, 1981).

19. Komiyama H., and Inoue H., Absorption of Nitrogen Oxides into Water. Chemical Engineering Science, 35, pp.154-161, (1980).

20. Sada E., and Kumazawa H., Absorption of NO in Aqueous Mixed Solutions of $NaClO_2$ and NaOH. Chemical Engineering Science, 33, pp.315-318, (1978).

21. Sada E., Kumazawa H., Yamanaka Y., Kudo I., and Kondo T., Kinetics of Absorption of Sulphur Dioxide and Nitric Oxide in Aqueous Mixed Solutions of Sodium Chlorite and Sodium Hydroxide. Journal of Chemical Engineering of Japan, 11, pp.276-282, (1978).

22. Danckwerts P.V., Gas-Liquid Reactions. pp.6,33,104, McGraw Hill Book Co., New York, (1970).

23. Wang J.C., and Himmelblau D.M., A Kinetic Study of Sulfur Dioxide in Aqueous Solution with Radioactive Tracers. A.I.Ch.E. Journal, 10, pp.574-580, (July, 1964).

24. Hikita H., Asai S., and Tsuji T., Absorption of Sulfur Dioxide into Aqueous Sodium Hydroxide and Sodium Sulfite Solutions. A.I.Ch.E.Journal, 23, pp.538-544, (July, 1977).

V. PROPOSED EXPERIMENTAL PROGRAM

A wet process is proposed for the simulation of the simultaneous removal of NO_x/SO_x. The NO_x/SO_x levels to be used in the experiments are based on the field sampling data given in Table 5-1. Experimental studies of the effects of scrubbing solution concentrations, pH values and ratios of liquid to gas flowrates are to be carried out on an absorption column which was designed earlier by Chen [1].

The removal of nitric oxide and sulphur dioxide from the gas stream by absorption in alkaline sodium chlorite solutions is to be investigated over a wide range of scrubbing liquor concentrations. Laboratory data will be developed to demonstrate the validity of the proposed models in order to provide a means of extrapolating this technique to commercial applications for simultaneous NO_x/SO_x removal.

The main elements of the system for this study consist of

1. feed system.
2. absorption column.
3. effluent system.
4. sampling system.

TABLE 5.1

Typical NO_x/SO_x Emission Levels and Flue Gas Compositions for Coal-Fired Boilers [2,3,4]

Furnace Outlet Temp. °C		Emission Level, ppm			
		NO_x		SO_x	
Range	Average	Range	Average	Range	Average
1093-1149	1122	164-1500	475	1400-1800	1562

Flue Gas Composition Components (Vol.%)								
N_2	O_2	CO_2	SO_2	SO_3	NO_x	HCl	H_2O	Particulate (dry basis*)
73.76	4.83	12.31	0.24	0.0024	0.06	0.01	8.79	6.65

* measured in g/scf (15.6 °C)

Detailed descriptions of each part of the overall system are provided in subsequent sections.

5.1 EXPERIMENTAL PLAN

Two sets of experiments are to be carried out with the absorption column operating under identical flow conditions. Studies will involve

1. physical absorption with water for the assessment of
   a) the removal of NO alone.
   b) the removal of SO_2 alone.
   c) the simultaneous removal of NO and SO_2.
2. chemical absorption with aqueous mixed sodium chlorite and sodium hydroxide solutions for the assessment of
   a) the removal of NO alone.
   b) the removal of SO_2 alone.
   c) the simultaneous removal of NO and SO_2.

5.1.1 Operating Condition

The scrubbing liquor is to be prepared from a 16% sodium chlorite solution which will be diluted to the desired concentrations ranging from 1% to 6% by weight. It has been shown that an increase in scrubbing liquor pH enhances the removal of NO_x/SO_x [5]. This condition is to be re-examined for the pH range 9 to 12, by addition of sodium hydroxide solution. The scrubbing liquid will be maintained at room

temperature whereas the flue gas is to be fed at temperatures ranging from 20 ^{o}C to 100^{o}C. For fixed inlet flue gas concentrations, the effect of scrubbing liquor flowrate on removal efficiency of NO_x/SO_x will be studied by varying the liquid-to-gas ratio over the range 10 to 20.

5.1.2 Wet Scrubbing Measurements

Flue gas concentrations in the feed stream are based on literature values as given in Table 5-1. The gas mixtures will consist of NO and SO_2.

5.1.2.1 The Absorption of NO or SO_2 alone

The inlet NO or SO_2 levels are to be controlled by a reducing valve on the NO or SO_2 cylinders. Inlet concentrations will be maintained at 500 ppm for NO and 1500 ppm for SO_2 during each run.

5.1.2.2 The Simultaneous Aborption of NO_x/SO_x

For the simultaneous absorption of NO_x/SO_x, the feed concentration of NO is to be varied from 160 ppm to 1500 ppm while the SO_2 level is fixed at 1500 ppm during each run. This range of inlet gas compositions is reasonable because over 95 per cent of the NO_x and SO_x in coal-fired flue gases is in the form nitric oxide and sulphur dioxide.

5.2 SCRUBBING SYSTEM

Figure 5-1 provides a schematic representation of the proposed experimental equipment. The basic apparatus consists of a feed system, absorption column, effluent system and sampling system.

5.2.1 Feed System

The feed system supplies air as diluent, scrubbing solution and a test flue gas from three separate units.

5.2.1.1 Air Supply Unit

The air supply unit consists an air blower which is capable of supplying up to 600 cfm of air at 33.7 inches of water static pressure. The flowrate of the air is controlled by a gate valve and is measured accurately by an orifice meter. The desired flue gas concentrations are set by adjusting the bypass which controls the air flowrate to the flue gas blending unit.

5.2.1.2 Scrubbing Liquor Supply Unit

Two-200 U.S. gallon plastic tanks are used to store the made-up alkaline chlorite liquor. This solution is delivered to the absorption column through a 1/2 inch flexible plastic hose by means of a bronze pump with a capacity of 11 gpm at 50 feet of head. The liquid flowrate is measured with a calibrated rotameter. It is further controlled by adjusting the re-circulation to the storage tank.

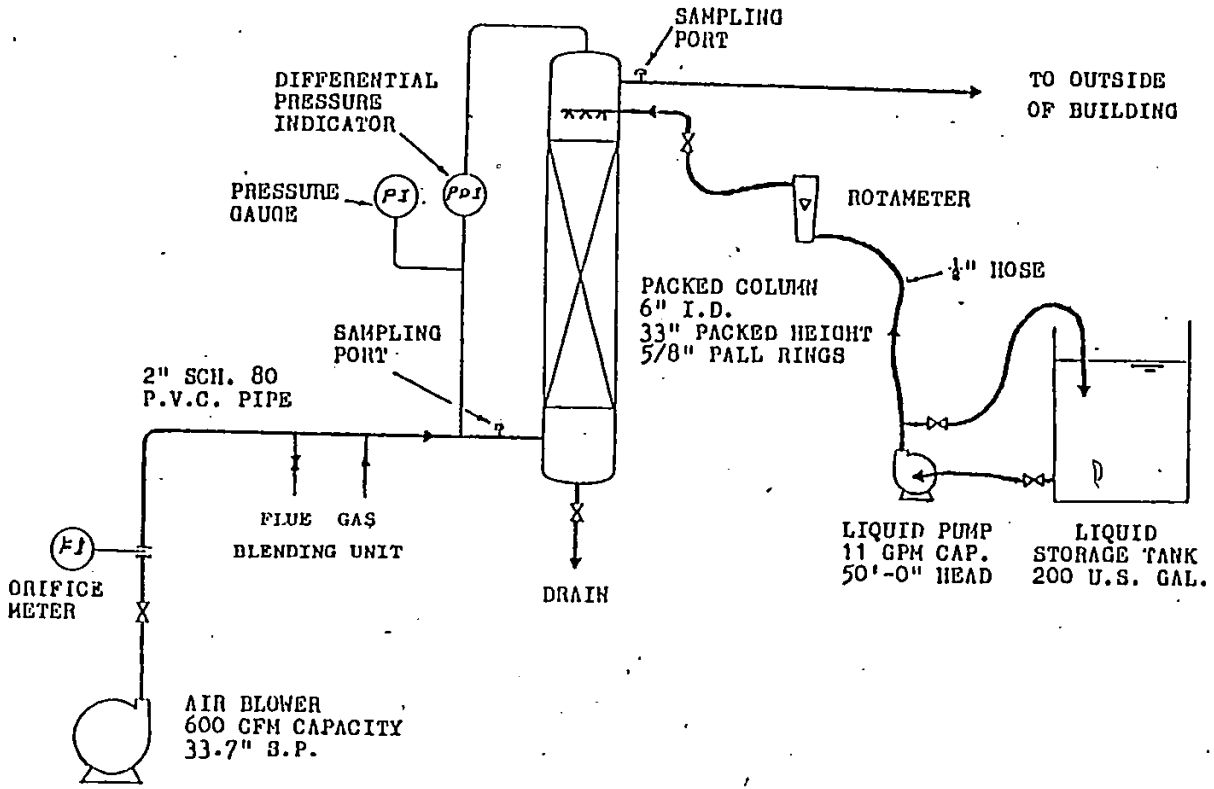

Figure 5-1. Schematic Diagram of Wet Scrubbing System (1)

5.2.1.3 Flue Gas Blending Unit

The blending unit is designed to produce a heated synthetic flue gas from various pure components contained in separate gas cylinders. The concentrations of NO and SO_2 can be varied over fairly wide ranges to approximate the values given in Table 5-1. Figure 5-2 provides a schematic representation of the gas blending unit. Prior to mixing, each gas is delievered through 0.25 inch o.d. stainless steel tubing to a calibrated rotameter for flow measurement.

Wet steam available in the laboratory is dried by passing it through heated aluminum coils. This dry, hot steam is then passed through a calibrated rotameter before mixing with the other components. Sulphur dioxide is fed into a common line which passes through the heated steam box where steam is added to the mixture after the NO and SO_2 are added. The entire gas mixture is then passed through a rotameter to determine the total flowrate. The synthetic flue gas is delivered through a main air line constructed of 2 inch schedule 80 PVC pipe to the absorption column.

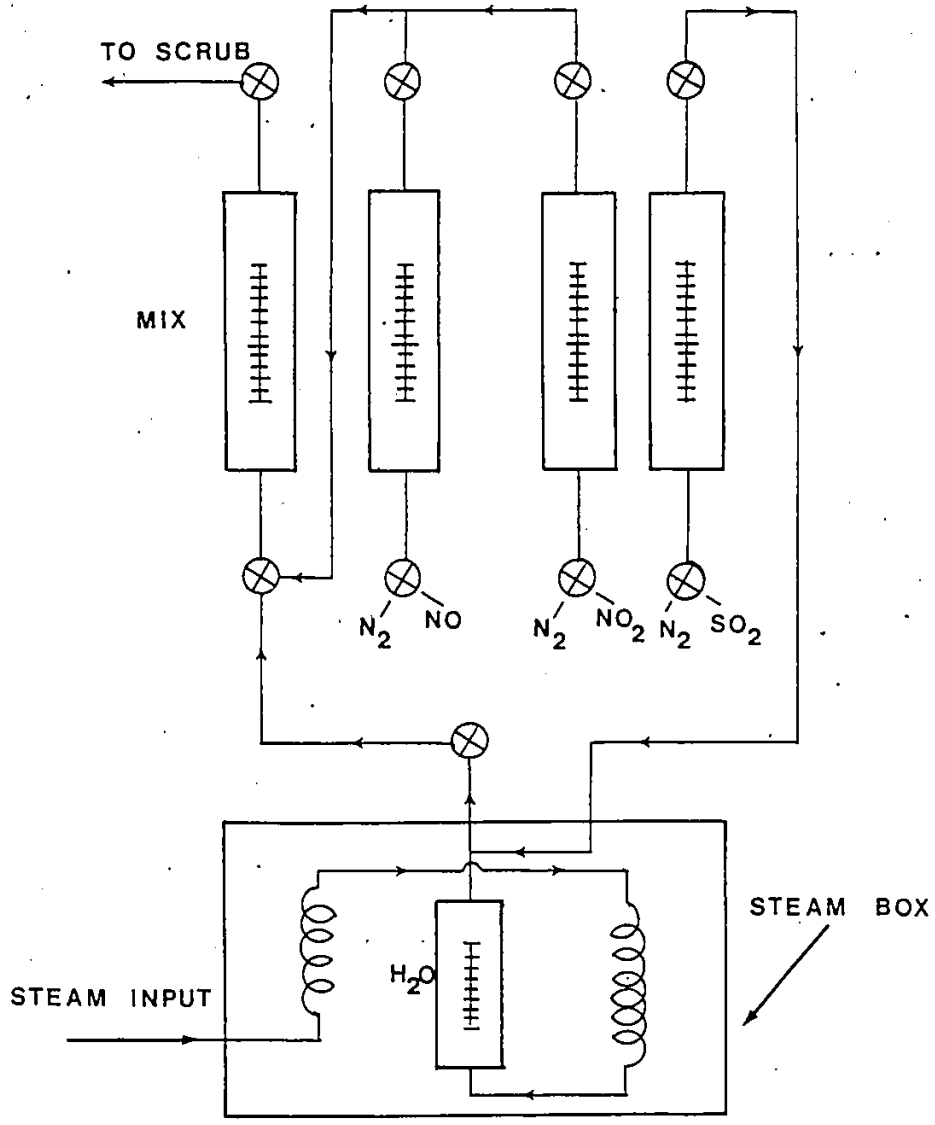

Figure 5-2 : Flue Gas Blending Unit (6)

5.2.2 Absorption Column

The absorption column to be used in this study consists of 6 inch I.D. Quickfit Pyrex glass sections. It is randomly packed with 5/8 inch stainless steel pall rings to a maximum height of 33 inches. The packing is supported on a teflon plate whose cross-section is drilled with holes to provide 70% void space. Alkaline sodium chlorite solution is fed over the top of the packed bed through a ring type sprayer. A demister is installed at the top of the column to remove water droplets which could interfere with the sampling system associated with the effluent NO_x /SO_x measurements.

The pressure difference between the inlet and outlet of the column is measured by a manometer. Air from the blower and flue gas from the blending unit are fed to the bottom of the packed column after the gas system is well mixed. Figure 5-3 shows construction details of the column.

5.2.3 Effluent System

Effluent gas is vented through a 2.5 inch plastic pipe to the outside of the building whereas the liquid effluent is collected in a surge tank and then discharged to the sewer system through a 2 inch flexible plastic garden-hose.

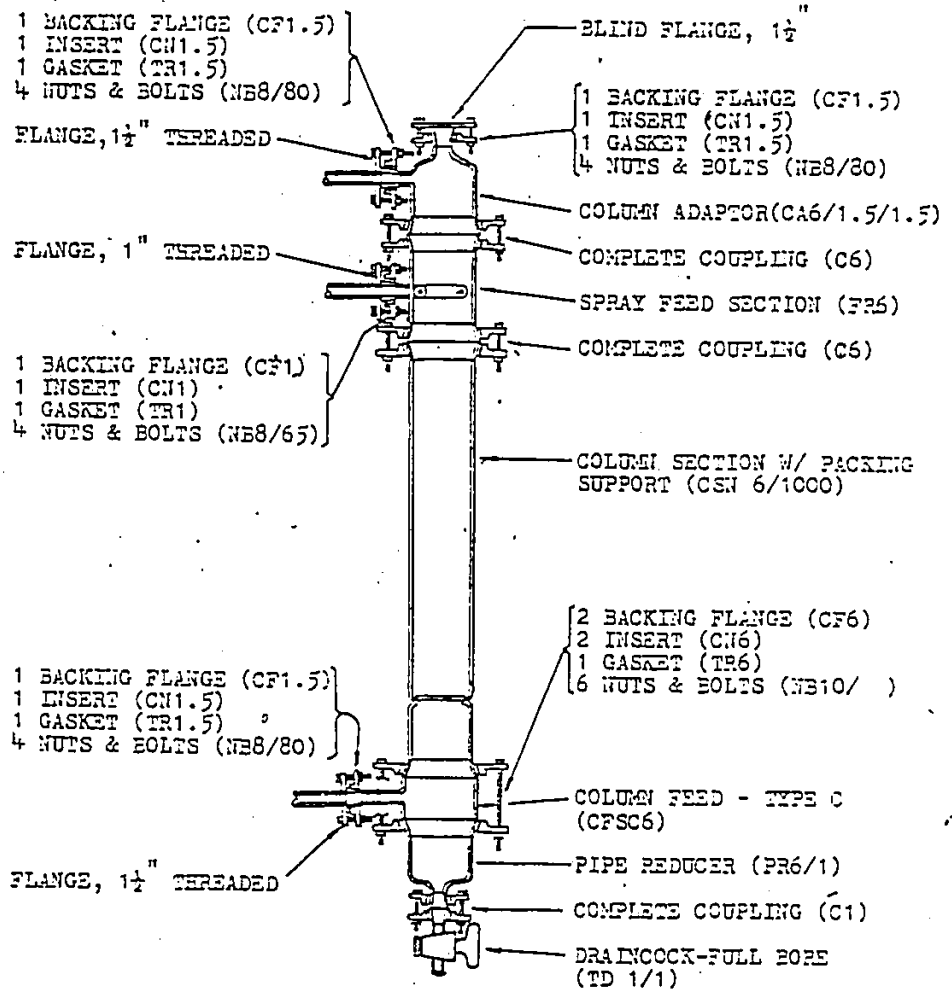

NOTE: ( ) - Q. V. F. CATALOG NO.

Figure 5-3 : Column Details (1)

5.2.4 Sampling System

A bypass section allows the inlet and outlet concentrations of NO_x /SO_x to be measured continuously by means of a Model NS-300 SO_2/ NO Analyzer. This NS-300 analyzer operates in a bimodular mode so that independent measurements for NO_x and SO_2 at inlet and outlet conditions are possible. Values obtained with the NS-300 analyzer at the outlet are to be checked further with an integrated manual impinger method [7]. Figure 5-4 shows a sketch of the sampling train. A pyrex wool plug is used in the probe to prevent water droplets from entering the gas bubblers. The gas bubblers are modified by replacing the orifice and impaction plates with semi-fine frits of approximately 70% porosity.

Since pressure drop across the gas bubblers is about ten inches of mercury, a check valve is provided in the system to prevent solution backup from the gas bubblers. Optimum sampling rates for maximum gas collection efficiency vary from 0.5 to 1.0 litres per minutes.

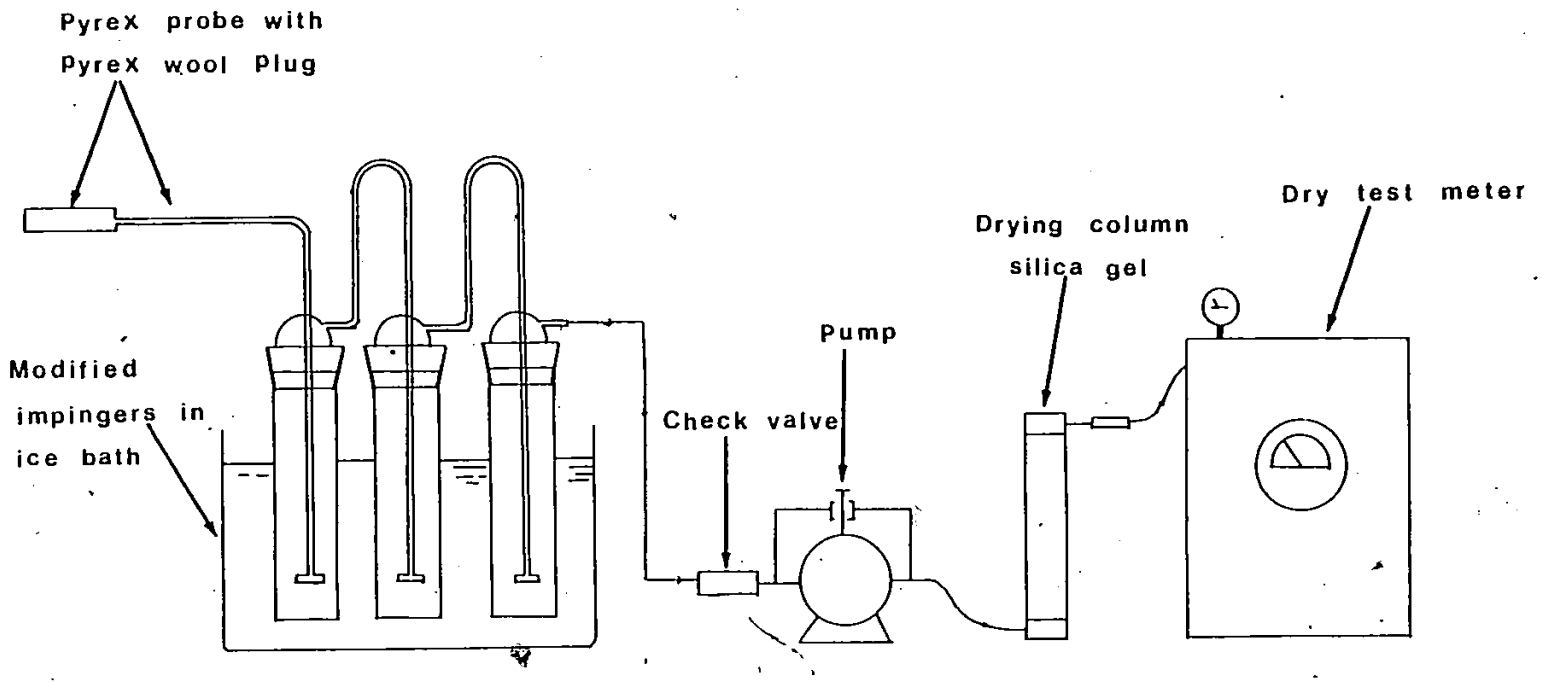

Figure 5-4 : Sampling Train (7)

REFERENCES

1. Chen R., Investigation of Odor Control by Alkaline Potassium Permanganate Solutions. M.A.Sc.Thesis, University of Windsor, Windsor, Ontario, (1978).

2. Siddiqi A.A., Control NO_x Emissions from Fixed Fireboxes. Hydrocarbon Processing, pp.94-97, (Oct. 1976).

3. McCann C.E., NO_x Emissions at Low Excess Air Levels in Pulverized-Coal Combustion. 70-WA/APC-3, The American Society of Mechanical Engineer, United Engineering Centre, 345 East 47 th Street, New York, N.Y. 10017, (August, 1970).

4. Yaverbaum L.H., Nitrogen Oxides Control and Removal, Recent Development. pp.8, Nyes Data Corporation, Park Ridge, New Jersey, U.S.A. (1979).

5. Takeuchi E., and Yamanaka Y., Simultaneous Absorption of SO_2 and NO_2 in Aqueous Solutions of NaOH and Na_2SO_3. Ind. Eng. Chem. Process Des. Dev. 17, No.14, pp.389-393, (1978).

6. Chappell G.A., Development of Aqueous Processes for Removing NO_x from Flue Gas. EPA-R2-72-051, Environmental Protection Agency, Washington, D.C., (September, 1972).

7. Levaggi D.A., An Integrated Manual Impinger Method for the Simultaneous Determination of NO_x and SO_x in Source Effluents. Journal of the Air Pollution Control Association, 26, pp.783-786, (1976).

VI. CONCLUSIONS AND RECOMMENDATIONS

6.1 CONCLUSIONS

The results of this investigation show that

1. adverse effects of NO_X/SO_X on human health and the environment have been confirmed. The acid rain problem experienced in many provinces of this country is the result of uncontrolled NO_X/SO_X emission.
2. Ontario is responsible for most of these toxic oxides of nitrogen emissions in comparision to other provinces.
3. about half of the Ontario NO_X emissions come from Ontario Hydro thermal power plants.
4. no emission control polices for NO_X have been instituted in this country.
5. the most effective way to reduce the NO_X/SO_X emission is to limit emissions from coal-fired thermal power stations.
6. combustion modification techniques and selective catalytic reduction methods are not suitable for handling coal derived NO_X/SO_X flue gases.
7. other techniques, such as electron beam radiation and adsorption by solids are in early stage of development and are not yet promising.

8. wet processes with dual NO_x /SO_x removal are more applicable to flue gases generated from coal-firing or high sulphur content oil burning processes.
9. alkaline sodium chlorite solution is recommended as a scrubbing solution on the basis of its technical and economic promises for industrial adaptation.

The second phase of this study was undertaken in order to develop a new model for predicting the rate of gas absorption in packed columns and to design, construct and test a continuous flue gas scrubbing system which would employ alkaline chlorite solution as the reactive absorbent. The proposed experimental program required the development of suitable analytical procedures that would insure accurate NO_x /SO_x material balances. The results of the second phase of this study show that

1. new models for physical absorption with water and chemical absorption with alkaline chlorite solution have been derived for the prediction of the rates of absorption in packed columns. A liquid residence time distribution function has been used to account for the semi-stagnant liquid pools in such columns.
2. the physical model is not limited to the NO_x/SO_x absorption problem but can be extended to any gaseous-liquid absorption in packed columns.
3. the chemical models are restricted to the NO_x /SO_x-(NaOH + $NaClO_2$) system by virtue of the reaction kinetics involved.

6.2 RECOMMENDATIONS FOR FUTURE WORK

Current studies have shown that the rates of absorption of NO_x/SO_x can be predicted for packed columns. Since literature values are not available to verify the proposed models, the following recommendations list the work which remains to be done:

1. obtain experimental data to verify the proposed models under various flow conditions.
2. determine the effect of varying the column packing height, superficial gas velocity, packing material and temperature of flue gas on absorption rates.
3. develop a computer program that will predict the rate of absorption for industrial conditions.
4. investigate solution regeneration techniques.

The final goal is to develop a viable process for the removal of NO_x/SO_x from coal-firing thermal power stations with solution regeneration as part of an integrated process that minimizes the impact of scrubbing products on the environment.

NOMENCLATURE

a = Interfacial area per unit column volume, $[m^2 . m^{-3}]$

$\bar{a}_L$ = Mean Stream interfacial area per unit liquid volume $[m^2 . m^{-3}]$

a_{Li} = Stream interfacial area per unit liquid volume, $[m^2 . m^{-3}]$

a_s = Geometric surface area per unit volume of packing particle, $[m^2 . m^{-3}]$

a_t = Total surface area of packing per unit column volume, $[m^2 . m^{-3}]$

a_w = Wetted surface area of packing per unit column volume, $[m^2 . m^{-3}]$

δa_i = Stream interfacial area per unit column volume, $[m^2 . m^{-3}]$

A = Absorbing gasesous component, (NO, NO_2, SO_2), dimensionless

B = Liquid reactant, (NaOH, $NaClO_2$), dimensionless

C_A ; C_A^* = Bulk and interfacial concentrations of the absorbing gaseous component A in liquid absorbent respectively $[Kmole . m^{-3}]$

$\bar{C}_{A,j-1}; \bar{C}_{A,j}$ = Mean concentration of component A in liquid phase leaving (j-1) th and j th stages respectively [Kmole.m^{-3}]

C_B^o = Initial liquid reactant concentration, [Kmole.m^{-3}]

$\bar{C}_{B,j-1}; \bar{C}_{B,j}$ = Mean liquid reactant concentration leaving (j-1) th and j th stages respectively, [Kmole.m^{-3}]

d = Nominal packing diameter, [m]

d_p = Diameter of a sphere having the same geometric surface area per unit volume of packing particle, [m] , $d_p = \frac{\{1 - \epsilon\}}{a_s}$

D_{AL} ; D_{AG} = Liquid phase and gas phase molecular diffusivities of gaseous component A respectively, [$m^2.s^{-1}$]

D = Axial dispersion coefficient, [$m^2.s^{-1}$]

Eö = Eotvos number, dimensionless , Eö = $\frac{\{\rho_L g d^2\}}{\sigma}$

E(t) = Residence time distribution function of liquid, [s^{-1}]

g = Acceleration due to gravity, [$m.s^{-2}$]

G = Superficial mass velocity of gas, [$Kg.m^{-2}.s^{-1}$]

$h_t; h_d; h_s$ = Total, dynamic and static liquid hold-up in a column respectively, [$m^3.m^{-3}$]

H = Henry's law constant for the absorbing component, [$atm.m^3.Kmole^{-1}$]

δh_i = Liquid hold-up for a stream i, [$m^3.m^{-3}$]

I_{B_1};I_{B_2} = Ionic strength of $NaClO_2$ and NaOH respectively, [Kg-ion.m^{-3}]

k_2 = Second order rate-constant for reaction of SO_2, [m^3.Kmole^{-1}.s^{-1}]

k_3 = Third order rate-constant for reaction of NO, [(m^3.Kmole^{-1})^2.s^{-1}]

k_G = Gas side mass transfer coefficient, [Kmole.m^{-2}.s^{-1}.atm^{-1}]

k_L = Liquid side mass transfer coefficient, [m.s^{-1}]

k_{Li} = Local liquid side mass transfer coefficient for a stream i, [m.s^{-1}]

k_{L,ClO_2^-} ; k_{L,OH^-} = Liquid side mass transfer coefficients of ClO_2^- and OH^- respectively, [cm.s^{-1}]

K_{B_1}; K_{B_2} = Salting-out parameters for the electrolytes, $NaClO_2$ and NaOH respectively, [m^3.Kmole^{-1}]

L = Superficial liquid mass velocity, [Kg.m^{-2}.s^{-1}]

M_{A_1} ; M_{A_2} = Parameters defined by Eqs.4-93 and 4-94 to characterise the process of absorption and reaction of two gases, dimensionless

n = Number of stages, dimensionless

N_A = Rate of absorption of component A, [Kmole.m^{-2}.s^{-1}]

P_t = Total pressure of the system, [atm]

P_A = Partial pressure of component A in bulk gas, [atm]

P_A^* = Partial pressure of component A at interface, [atm]

Pe = Peclet number based on packing, dimensionless

$$Pe = \frac{\bar{U}d}{\mathbb{D}}$$

q_{A_1} ; q_{A_2} ; $q_{A_1A_2}$ = Parameters defined by Eqs. 4-95, 4-96, and 4-97 to characterise the process of absorption of two gases, (SO_2, NO), dimensionless

Q = Volumetric flowrate of liquid absorbent in a column, $[m^3.s^{-1}]$

δq_i = Volumetric flowrate for a stream i, $[m^3.s^{-1}]$.

r = Local rate of reaction, $[Kmole.m^{-3}.s^{-1}]$

R = Gas constant, $[atm.m^3.Kmole^{-1}.{}^oK^{-1}]$

S = Column cross sectional area, $[m^2]$

S_p = Specific surface of a particle, $[m^2.m^{-3}]$

t_i = Stream residence time, [s]

$\bar{t}$ = Mean residence time, [s]

t = Contact-time, [s]

T = Absolute temperature, $[{}^oK]$

$\bar{U}$ = Mean real liquid velocity, $[m.s^{-1}]$, $\bar{U} = \frac{Q \epsilon h_t}{S}$

v_L = Liquid velocity, $[m.s^{-1}]$, $v_L = \frac{Q}{S}$

x = Distance beneath liquid surface, [m]

$x_a; x_c; x_g$ = Contribution to salting-out parameter K, of anions, cations and the gas respectively, [$m^3 \cdot Kg\text{-}ion^{-1}$]

Y_A = Molar fraction of absorbing component A, dimensionaless

Y_A^* = Molar fraction of absorbing component A at interface in equilibrium with C_A^*, dimensionless

$\bar{Y}_{A,j}$ = Mean molar fraction of absorbing component A defined by Eq. 4-28, dimensionless

Z = Total height of packing, [m]

ΔZ = Height of a stage, [m]

Greek Symbols:

β = Liquid fraction passing through the stagnant region, dimensionless

$\mathcal{E}$ = Parameter used to account for the various hydrodynamic conditions in a column, [$m.s^{-\frac{1}{2}}$]

δ = Effective liquid film thickness, [m]

ϵ = Porosity, (void fraction), dimensionless

θ = Exposure time, [s]

λ = Defined by Eq. 4-52, [m]

μ = Dynamic viscosity, [$Kg.m^{-1}.s^{-1}$]

$\mathcal{F}$ = Stoichiometric coefficients, dimensionless

ψ_i = Valency of ion, dimensionless

ρ = Density , [$Kg.m^{-3}$]

σ = Surface tension of liquid, [$N.m^{-1}$] or [$Kg.s^{-2}$]

σ_c = Critical surface tension of packing material, [$N.m^{-1}$] or [$Kg.s^{-2}$]

Γ_1 ; Γ_2 = Mean residence time of liquid, defined by Eqs 4-9 and 4-10 respectively, [s]

$\emptyset$ = Mass transfer enhancement factor, dimensionless

$\Phi_1;\Phi_2;\Phi_3;\Phi_4$ = Defined by Eqs. 4-103, 4-104, 4-105, 4-106, respectively.

Subscripts;

A = Flue gas component A

A_1 ; A_2 = Dissovlved flue gas component (SO_2 and NO respectively)

B = Liquid reactant B

B_1 ; B_2 = Liquid phase reactant ($NaClO_2$ and NaOH respectively)

Chem = Chemical absorption

i = Referring to stream i

j = Referring to stage j

L = Liquid phase

G = Gas phase

Phy = Physical absorption

Appendix A

SOLUBILITY AND DIFFUSIVITY

According to Sada et al.[1], the interfacial concentrations of sulphur dioxide or nitric oxide ($J = C^*_{A_1}$; $C^*_{A_2}$) in aqueous mixed solutions of sodium hydroxide and sodium chlorite can be estimated from the correlation of gas solubility in mixed electrolyte solutions [2] expressed by

$$\log \left\{ \frac{C^*_J}{C_{J,water}} \right\} = - \left\{ K_{B_1} I_{B_1} + K_{B_2} I_{B_2} \right\} \qquad \text{----(A-1)}$$

where K_{B_1} and K_{B_2} are the salting-out parameters for the electrolyte B_1 ($NaClO_2$) and B_2 (NaOH) respecively. The magnititude of a salting-out parameter depends on the ion and gas present and is given by

$$K = \left\{ x_g + x_a + x_c \right\} \qquad \text{-------(A-2)}$$

The values of x for various species are listed in Table A-1. The symbols I_{B_1} and I_{B_2} represent the ionic strength of sodium chlorite ($NaClO_2$) and sodium hydroxide (NaOH) respectively according to

$$I = \tfrac{1}{2} \sum_i^n C_i \psi_i^2 \qquad \text{------(A-3)}$$

TABLE A.1

Values of x for Various Species [1,2,5]

Species	x_g	x_a $[m^3.Kg\text{-}ion^{-1}]$	x_c
NO (25°C)	-0.1825	---	---
SO_2 (25°C)	-0.3145	---	---
OH^-	---	0.3875	---
ClO_2^-	---	0.3497	---
Na^+	---	---	-0.0183

where C_i represents the concentration of ions of valency ψ_i. The interfacial concentration of sulphur dioxide in water, $C^*_{A_1,water}$, in equilibrium at pressure $P^*_{A_1}$ is evaluated using the Rabe and Harris [6,7] Equation in the form of Henry's law constant for nonionized sulphur dioxide given by

$$H_{A_1} = \exp\left\{\frac{2851.1}{T} - 9.3795\right\} \qquad \text{.....(A-4)}$$

where H_{A_1} is the Henry's law constant in [g-mol.bar^{-1}.l^{-1}] and T is the temperature in ^oK. On this basis the concentration of nonioized sulphur dioxide in pure water can be obtained from

$$C^*_{A_1,water} = P_{A_1} H_{A_1} \qquad \text{.....(A-5)}$$

where P_{A_1} is the partial presure of SO_2 in the gas phase. The interfacial concentration of nitric oxide, $C^*_{A_2,water}$, is estimated from

$$C^*_{A_2,water} = P_{A_2} H_{A_2} \qquad \text{.....(A-6)}$$

where H_{A_2} is available in the literature [1] and is equal to $1.92*10^{-6}$ (mol.cm^{-3}.atm^{-1}) at 25 ^oC.

The liquid phase diffusivity of nitric oxide, D_{A_2L}, is estimated from the equation proposed by Joosten and Danckwerts [1,3] in the form

$$\left\{\frac{D}{D_{water}}\right\}_{NO} = \left\{\frac{D}{D_{water}}\right\}_{N_2O} \qquad \text{.....(A-7)}$$

The value of D_{water} for NO in water is available in the literature [1,4] ($2.53*10^{-5}$ [$cm^2.s^{-1}$] at 25 ^oC). The diffusivity of nitrous oxide in mixed salt salutions is given in Table A-2, whereas the value for N_2O in water is $1.92*10^{-5}$ [$cm^2.s^{-1}$] at 25 ^oC [3].

The liquid phase diffusivity of sulphur dioxide, D_{A_1L}, in aqueous solutions is available in literature [1], (D_{A_1L} = $1.90*10^{-5}$ $cm^2.s^{-1}$ at 25 ^oC).

TABLE A.2

Diffusivity of Nitrous Oxide in Aqueous Mixed Solution of $NaClO_2$ and NaOH Derived from Physical Absorption Data with a Laminar Liquid-Jet at 1 Atm and 25 °C [1]

Sodium Chlorite Concentration [mol/l]	Sodium Hydroxide Concentration [mol/l]	Diffusivity of Nitrous Oxide [cm^2/sec]
0.00	0.00	$1.66*10^{-5}$
0.25	0.10	$1.62*10^{-5}$
0.50	0.10	$1.60*10^{-5}$
1.00	0.10	$1.57*10^{-5}$
1.50	0.10	$1.52*10^{-5}$
2.00	0.10	$1.46*10^{-5}$
1.00	0.20	$1.58*10^{-5}$
1.00	0.50	$1.23*10^{-5}$
1.00	0.70	$9.48*10^{-6}$

REFERENCES

1. Sada E., Kumazawa H., Yamanaka Y., Kudo I., and Kondo I., Kinetics of Absorption of Sulphur Dioxide and Nitric Oxide in Aqueous Mixed Solutions of Sodium Chlorite and Sodium Hydroxide. Journal of Chemical Engineering of Japan, 11, pp.276-282, (1978).

2. Onda K., Sada E., Kobayashi T., Kito S., and Ito K., Solubility of Gases in Aqueous Solutions of Mixed Salts. Journal of Chemical Engineering of Japan, 3, pp.137-142, (1970).

3. Joosten G.E.H., and Danckwerts P.V., Solubility and Diffusivity of Nitrous Oxide in Equimolar Potassium Carbonate - Potassium Bicarbonate Solutions at 25 °C and 1 Atmosphere. Journal of Chemical and Engineering Data, 17, pp.452-454, (1972).

4. Wise D.L., and Houghton G., Diffusion Coefficients of Neon, Krypton, Xenon, Carbon Monoxide and Nitric Oxide in Water at 10 - 60 °C. Chemical Engineering Science, 23, pp.1211-1216, (1968).

5. Sada E., and Kumazawa H., Absorption of NO in Aqueous Mixed Solutions of $NaClO_2$ and NaOH. Chemical Engineering Science, 33, pp.315-318, (1978).

6. Chang C.S., and Rochelle, SO_2 Absorption into Aqeous Solutions - A.I.Ch.E. Journal, 27, pp.292-298, (March, 1981).

7. Rabe A.E., and Harris J.F., Vapour Liquid Equilibrium Data for the Binary System, Sulfur Dioxide and Water. Journal of Chemical and Engineering Data, 8, pp.333, (1963).

VITA

Mr. Kam Foon Chan was born in People's Republic of China on Nov. 12, 1955. Mr. Chan received his B.A.Sc. (Hon.) in Chemical Engineering from the University of Windsor, Ontario, Canada. He is currently a master candidate in the Department of Chemical Engineering, University of Windsor, Windsor, Ontario, Canada.